Eur. Phys. J. C (2026) 86:210
https://doi.org/10.1140/epjc/s10052-026-15408-6

THE EUROPEAN PHYSICAL JOURNAL C

Regular Article - Theoretical Physics

Loop-corrected trilinear Higgs self-couplings in the NMSSM with inverse seesaw mechanism

Thi Nhung Dao[1,a], **Martin Gabelmann**[2,b], **Margarete Mühlleitner**[3,c]

[1] Phenikaa Institute for Advanced Study, PHENIKAA University, Hanoi 12116, Vietnam
[2] Albert-Ludwigs-Universität Freiburg, Physikalisches Institut, Hermann-Herder-Str. 3, 79104 Freiburg, Germany
[3] Institute for Theoretical Physics, Karlsruhe Institute of Technology, Wolfgang-Gaede-Str. 1, 76131 Karlsruhe, Germany

Received: 10 July 2025 / Accepted: 7 February 2026

Abstract The higher-order corrections for the SM-like Higgs boson mass and the trilinear Higgs self-couplings in the Next-to-Minimal Supersymmetric extension of the Standard Model (NMSSM) with Inverse Seesaw Mechanism are significant and highly correlated. We present here the full one-loop corrections to the trilinear Higgs self-couplings supplemented by the dominant top-Yukawa and strong coupling induced two-loop corrections from our previous calculations in the complex NMSSM. These corrections are performed consistently with the corresponding Higgs boson mass corrections. We discuss in detail the new effects from the extended neutrino and sneutrino sectors on both the trilinear Higgs self-couplings and the SM-like Higgs boson mass. When compared to the case of the NMSSM without Inverse Seesaw Mechanism, the new effects can be up to 10% for the effective SM-like trilinear Higgs self-couplings, and up to 4.5% for the SM-like Higgs boson mass for valid parameter points, i.e. points satisfying the Higgs data, the neutrino data, the constraints from the charged lepton flavor-violating decays, and the new physics constraints from the oblique parameters S, T, U. The new corrections are also included in the Higgs-to-Higgs decays for the heavy Higgs states and implemented in the new version of the Fortran code `NMSSMCALC-nuSS`.

1 Introduction

The Standard Model (SM) has been shown to describe the world of particle physics successfully at the highest precision. Moreover, it has been structurally completed with the discovery of the Higgs boson by the Large Hadron Collider (LHC) collaborations ATLAS and CMS in 2012 [1,2]. The subsequent measurements of the properties of the discovered particle are consistent with the predictions of the SM [3,4]. Despite its success, the SM cannot explain certain phenomena. Among these are the explanation of the tiny non-zero neutrino masses, the existence of Dark Matter (DM), and the observed baryon asymmetry of the Universe. The SM needs to be extended in both its particle content and symmetry principles in order to address these questions. In the SM, neutrinos are massless since only left-handed neutrino components are included. The Higgs sector is minimal, consisting of only one Higgs doublet. There is no interaction between the Higgs boson and neutrinos. The Higgs and the neutrino sector, hence, do not have an impact on each other. The situation changed with the discovery of the neutrino masses [5]. The need to accommodate non-zero neutrino masses requires an enlarged neutrino sector, implying interactions between neutrinos and the Higgs boson. In line with the Higgs mechanism for the generation of particle masses, the tiny neutrino masses would lead to tiny neutrino Yukawa couplings. This is, however, not the case in the so-called inverse seesaw mechanism, [6,7], which allows for possibly large couplings. In this situation, one can expect a significant interplay between the two sectors and noticeable impacts of the neutrino sector on the Higgs observables.

Supersymmetric theories [8–21] belong to the most intensely studied and best-motivated theories beyond the SM that potentially solve the most pressing open questions cited above. They require an extended Higgs sector entailing an enlarged Higgs spectrum with an interesting phenomenology. Calculations performed within supersymmetry can be transferred to other benchmark models with extended Higgs sectors that are tested by experiment, like e.g. the 2-Higgs-

[a] e-mail: nhung.daothi@phenikaa-uni.edu.vn (corresponding author)
[b] e-mail: martin.gabelmann@physik.uni-freiburg.de
[c] e-mail: margarete.muehlleitner@kit.edu

Published online: 02 March 2026

Doublet Model (2HDM), with a minimum of effort. In supersymmetry, the mass of the SM-like Higgs boson is not a free parameter. It is obtained from the supersymmetric input parameters, and higher-order corrections are crucial in this context to obtain a Higgs mass value that is compatible with the 125 GeV mass measured by the LHC experiments (for recent reviews, see [22,23]). Precision calculations of the Higgs mass combined with precision measurements consequently allow us to restrict the allowed parameter space of supersymmetry and further pin down a more-fundamental theory describing nature.

Investigations of the heavy neutrino impact on the SM-like Higgs boson mass have been performed in some supersymmetric extensions. In the Minimal Supersymmetric Standard Model (MSSM) [24–27] extended by the seesaw mechanism, the corrections stemming solely from the heavy neutrinos and their superpartners can be several GeV, cf. [28–33]. The MSSM extended by a complex singlet field, the so-called next-to-Minimal Supersymmetric Standard Model (NMSSM) [11,14,16,17,34–45], solves the $\mu-$problem and provides with its non-minimal Higgs sector and larger neutralino sector a rich phenomenology [46,47]. The NMSSM, with an extended neutrino sector, can have a significant impact on the SM-like Higgs boson mass, as shown in [48–50]. Recently, our group has also contributed to the investigation of the Higgs boson mass in the context of extended Higgs sectors in supersymmetric theories. We have calculated in [51] the full one-loop corrections in the complex NMSSM extended by six singlet leptonic superfields together with the dominant two-loop corrections computed at $\mathcal{O}(\alpha_t^2)$ in the limit of the complex MSSM and the $\mathcal{O}(\alpha_t\alpha_s)$ corrections in the vanilla complex NMSSM. We found that the impact of these singlet superfields on the h_u-like Higgs boson[1] can be of up to 5 GeV, taking into account the constraints from Higgs data, active light neutrino data, oblique parameters, and lepton flavor violation decays such as $\mu \to e\gamma$ and $\tau \to e\gamma$, $\tau \to \mu\gamma$. We have furthermore found significant effects of the extended (s)neutrino sector on the muon/electron anomalous magnetic moment (AMM), as shown in [52], where we also computed the impact on the electric dipole moment. All our calculations have been implemented in the public `Fortran` code `NMSSMCALC-nuSS`, which computes the Higgs boson masses and mixings as well as the Higgs boson decay widths and branching ratios, taking into account the state-of-the-art higher-order QCD corrections. The code furthermore calculates the electric dipole moment and the anomalous magnetic moment of charged leptons, including the full one-loop and the dominant two-loop corrections.

The ultimate confirmation that the Higgs mechanism is responsible for mass generation is given by the reconstruction of the Higgs potential itself. This requires the measurement of the Higgs self-couplings [53–55]. At the LHC the trilinear Higgs coupling (THC) is directly accessible in Higgs pair production through gluon fusion at hadron colliders [54,56] and in double Higgs strahlung and W boson fusion into Higgs pairs at e^+e^- colliders [53]. The Higgs boson couplings to the SM particles have been measured to be SM-like. The current experimental constraints at 95% CL on the THC modifier κ_λ, given by the ratio of the SM-like THC in the new physics model λ_{hhh} to the tree-level THC $\lambda^{(0)}_{\rm SM}$ of the SM, $\kappa_\lambda \equiv \lambda_{hhh}/\lambda^{(0)}_{\rm SM}$, on the other hand, are still rather loose, with $-1.2 < \kappa_\lambda < 7.2$ given by ATLAS [57] and $-1.24 < \kappa_\lambda < 6.9$ given by CMS [4], assuming a SM top-quark Yukawa coupling. There is hence still room for beyond-SM physics in the THC [58]. In the high-luminosity phase of the LHC, it is expected that the sensitivity range can be reduced to $-0.5 < \kappa_\lambda < 1.6$ [59], at high-energy linear colliders a 10–20% accuracy can be reachable, see e.g. Refs. [60–62], and at the high-luminosity 100 TeV hadron collider the THC can be measured with about 3.5–8% accuracy [63]. This requires precise theoretical predictions of the THC in the SM as well as models beyond the SM. Moreover, the Higgs boson mass and the THC are intimately related through the Higgs potential. For the consistent interpretation of the experimental results, the predictions for the Higgs boson mass and the trilinear Higgs self-coupling hence have to be provided by theory at the same precision. Deviations of the THC from the SM value lift the destructive interference between the triangle and box diagrams contributing to gluon fusion Higgs pair production at the LHC. The impact of potentially large higher-order corrections and interference effects on the comparison between the experimental results and the theoretical predictions for Higgs boson pair production at the LHC can therefore be substantial [64–66].

In the SM, the tree-level THC $\lambda^{(0)}_{\rm SM}$ is uniquely determined by the Higgs boson mass M_H as $\lambda^{(0)}_{\rm SM} = 3M_H^2/v$, where $v \approx 246$ GeV denotes the vacuum expectation value. In the on-shell scheme, the dominant one-loop corrections [67] and the dominant two-loop corrections [68,69] arising from the top-quark Yukawa coupling are of about -8.5% and $+1.4\%$, respectively. In the MSSM, the one-loop corrections to the effective trilinear couplings have been provided many years ago in [67,70,71]. The process-dependent corrections to heavy scalar MSSM Higgs decays into a lighter Higgs pair have been calculated in [72,73]. The two-loop $\mathcal{O}(\alpha_t\alpha_s)$ SUSY-QCD corrections to the top/stop-loop induced corrections have been made available within the effective potential approach in [74]. In the NMSSM, we provided the full one-loop corrections for the CP-conserving NMSSM [75]. They

[1] The Higgs boson with dominant up-type-like doublet component h_u behaves like the SM Higgs.

are sizeable so that the inclusion of the two-loop corrections is mandatory to reduce the theoretical uncertainties due to missing higher-order corrections. Consequently, we subsequently calculated the two-loop $\mathcal{O}(\alpha_t\alpha_s + \alpha_t^2)$ corrections in the limit of vanishing external momenta in [76,77], in the CP-violating NMSSM. The full one-loop corrections to the Higgs-to-Higgs decays and other on-shell two-body decays were implemented in [78]. For corrections to the trilinear Higgs self-couplings in non-supersymmetric (non-SUSY) Higgs models, see for example Refs. [79–87] for one-loop and Refs. [68,69,88–91] for two-loop results, and Refs. [92–101] for the process-dependent Higgs-to-Higgs decays at one-loop level.

In this paper, we extend the computation of the higher-order corrections from the masses to the trilinear Higgs self-couplings in the framework of the complex NMSSM with the inverse see-saw mechanism as a benchmark model that, as a SUSY model, allows for the solution of several open problems of the SM and, with its inverse see-saw mechanism, allows for an explanation of massive neutrinos. Since the effect of the extended (s)neutrino sector on the mass can be significant, as we found in [51], where we calculated the full one-loop corrections to the Higgs boson mass consistently combined with the dominant Yukawa and strong coupling induced two-loop corrections, sizable effects on the THC can be expected as well. In a simple extension of the SM including one Dirac heavy neutrino, the impact of the one heavy neutrino on the SM THC has been investigated in [102]. It can be of order +20% to +30% if the off-shell Higgs momentum is fixed to $q_H^* = 2500\,\text{GeV}$. The conclusion is further confirmed in the SM with the inverse seesaw mechanism, provided that the magnitude of the neutrino Yukawa coupling $|Y_\nu| > 3$ [103].

Furthermore, we quantify the effect of the (s)neutrinos on the THCs when including higher-order corrections and investigate their correlation with the previously computed higher-order corrections to the Higgs boson masses, taking into account the current constraints from the LHC Higgs data, from active neutrino data as well as the LHC constraints on the search for electroweakinos, charged sleptons and sneutrinos. In detail, we compute the full one-loop corrections from all sectors of the model to the THCs taking into account the full dependence on external momenta. Furthermore, we factorize the dominant corrections from the (s)top sector and the heavy neutrinos and their superpartners and then include them to the effective trilinear Higgs self-couplings which are defined at the zero external momentum. Additionally, to improve the accuracy of the theoretical predictions for the THCs and the Higgs-to-Higgs decays, we include also the dominant top-Yukawa (α_t) and strong coupling (α_s) induced two-loop corrections of the order $\mathcal{O}(\alpha_t(\alpha_s + \alpha_t))$ from our previous calculations [76,77] in the complex NMSSM. Our results are implemented in the new version of the code `NMSSMCALC-nuSS`.

The outline of the paper is as follows. In Sect. 2 we introduce the NMSSM with the inverse seesaw mechanism at tree level and set our notation. In Sect. 3 we describe our computation of the electroweak one-loop corrections to the THCs. In the numerical results presented in Sect. 4 we analyze the impact of the (s)neutrino sector on the THCs in comparison with their impact on the SM-like Higgs boson mass. Furthermore, we investigate the electroweak corrections as a function of the relevant (s)neutrino sector parameters and discuss scatter plots obtained from the parameter scan. In Sect. 5 we summarize our results.

2 The model at tree level

We consider the complex NMSSM with inverse seesaw mechanism, abbreviated as NMSSM-nuSS. Its main differences compared to the usual complex NMSSM are in the neutrino and sneutrino sectors. We have introduced the model in detail in our previous studies [51,52]. In the following, we only give a short introduction into the model and refer the reader to [51,52] for a detailed discussion.

The NMSSM-nuSS extends the complex NMSSM by including six gauge-singlet chiral superfields $\hat{N}_i$, $\hat{X}_i$ ($i = 1, 2, 3$) that carry lepton number. We further impose a discrete $\mathbb{Z}_3$ symmetry with a unit charge of $\omega = e^{i2\pi/3}$ on the NMSSM-nuSS. With the particular $\mathbb{Z}_3$ charge assignment presented in [51] we find the following NMSSM-nuSS superpotential[2]

$$\begin{aligned}\mathcal{W}_{\text{NMSSM-nuSS}} = W_{\text{MSSM}} - \epsilon_{ab}\lambda\hat{S}\hat{H}_d^a\hat{H}_u^b + \frac{1}{3}\kappa\hat{S}^3 \\ - y_\nu\epsilon_{ab}\hat{H}_u^a\hat{L}^b\hat{N}^c + \lambda_X\hat{S}\hat{X}\hat{X} + M_X\hat{X}\hat{N}^c\,,\end{aligned} \tag{1}$$

where the complex MSSM superpotential is given by

$$\mathcal{W}_{\text{MSSM}} = -\epsilon_{ab}\left(y_u\hat{H}_u^a\hat{Q}^b\hat{U}^c - y_d\hat{H}_d^a\hat{Q}^b\hat{D}^c - y_e\hat{H}_d^a\hat{L}^b\hat{E}^c\right)\,. \tag{2}$$

In the above expressions, the quark and lepton superfields are denoted by $\hat{Q}$, $\hat{U}$, $\hat{D}$ and $\hat{L}$, $\hat{E}$, respectively, whereas the Higgs doublet superfields are $\hat{H}_d$, $\hat{H}_u$ and the singlet superfield is $\hat{S}$. The totally antisymmetric tensor is given by $\epsilon_{12} = \epsilon^{12} = 1$. Charge conjugated fields are denoted by the superscript c. Color and generation indices have been omitted. The quark and lepton Yukawa couplings y_d, y_u, y_e

[2] In comparison with [51,52] we have changed the notation of μ_X to M_X.

are chosen to be real and diagonal. However, the coupling and mass matrices in the neutrino sector, y_ν, λ_X, M_X, are in general non-diagonal and complex. The NMSSM-specific coupling parameters λ and κ are complex. The soft SUSY-breaking NMSSM-nuSS Lagrangian respecting the gauge symmetries and the global $\mathbb{Z}_3$ symmetry reads

$$\begin{aligned}\mathcal{L}^{\text{soft}}_{\text{NMSSM-nuSS}} = \mathcal{L}^{\text{soft}}_{\text{NMSSM}} &+ (\epsilon_{ab} y_\nu A_\nu H_u^a \tilde{L}^b \tilde{N}^* \\ &+ \lambda_X A_X S \tilde{X}\tilde{X} + \mu_X B_{\mu_X} \tilde{X}\tilde{N}^* + h.c.) \\ &- \tilde{m}_X^2 \left|\tilde{X}\right|^2 - \tilde{m}_N^2 \left|\tilde{N}\right|^2 \,, \end{aligned} \tag{3}$$

with the neutrino trilinear couplings A_ν, A_X and the bilinear mass B_{μ_X}. The soft SUSY-breaking mass parameters $\tilde{m}_X^2, \tilde{m}_N^2$ are 3×3 matrices and the soft SUSY-breaking NMSSM Lagrangian is

$$\begin{aligned}\mathcal{L}_{\text{soft,NMSSM}} = &-m_{H_d}^2 H_d^\dagger H_d - m_{H_u}^2 H_u^\dagger H_u - m_{\tilde{Q}}^2 \tilde{Q}^\dagger \tilde{Q} \\ &- m_{\tilde{L}}^2 \tilde{L}^\dagger \tilde{L} - m_{\tilde{u}_R}^2 \tilde{u}_R^* \tilde{u}_R - m_{\tilde{d}_R}^2 \tilde{d}_R^* \tilde{d}_R \\ &- m_{\tilde{e}_R}^2 \tilde{e}_R^* \tilde{e}_R - (\epsilon_{ij}[y_e A_e H_d^i \tilde{L}^j \tilde{e}_R^* \\ &+ y_d A_d H_d^i \tilde{Q}^j \tilde{d}_R^* - y_u A_u H_u^i \tilde{Q}^j \tilde{u}_R^*] + \text{h.c.}) \\ &- \frac{1}{2}(M_1 \tilde{B}\tilde{B} + M_2 \tilde{W}_j \tilde{W}_j + M_3 \tilde{G}\tilde{G} + \text{h.c.}) \\ &- m_S^2 |S|^2 + (\epsilon_{ij} \lambda A_\lambda S H_d^i H_u^j - \frac{1}{3}\kappa A_\kappa S^3 + \text{h.c.}) \,. \end{aligned} \tag{4}$$

We treat all soft SUSY-breaking gaugino mass parameters, M_k ($k = 1, 2, 3$), of the bino, wino and gluino fields, $\tilde{B}$, $\tilde{W}_l$ ($l = 1, 2, 3$) and $\tilde{G}$, respectively, as well as the soft SUSY-breaking trilinear couplings, A_x ($x = \lambda, \kappa, u, d, e$), as complex. In this model, there are only two lepton number violating terms, namely $\lambda_X \hat{S}\hat{X}\hat{X}$ and $\lambda_X A_X S \tilde{X}\tilde{X}$.

The tree-level Higgs potential is given by

$$\begin{aligned} V_H = &(|\lambda S|^2 + m_{H_d}^2) H_d^\dagger H_d + (|\lambda S|^2 + m_{H_u}^2) H_u^\dagger H_u + m_S^2 |S|^2 \\ &+ \frac{1}{8}(g_2^2 + g_1^2)(H_d^\dagger H_d - H_u^\dagger H_u)^2 + \frac{1}{2} g_2^2 |H_d^\dagger H_u|^2 \\ &+ |-\epsilon^{ij} \lambda H_{d,i} H_{u,j} + \kappa S^2|^2 + \big[-\epsilon^{ij} \lambda A_\lambda S H_{d,i} H_{u,j} \\ &+ \frac{1}{3}\kappa A_\kappa S^3 + \text{h.c.}\big], \end{aligned} \tag{5}$$

where g_1 and g_2 denote the $U(1)_Y$ and $SU(2)_L$ gauge couplings, respectively. Electroweak symmetry breaking (EWSB) occurs at the minimum of the Higgs potential where the three neutral Higgs boson fields acquire non-vanishing VEVs,

$$H_d = \begin{pmatrix} \frac{v_d + h_d + i a_d}{\sqrt{2}} \\ h_d^- \end{pmatrix}, \quad H_u = e^{i\varphi_u} \begin{pmatrix} h_u^+ \\ \frac{v_u + h_u + i a_u}{\sqrt{2}} \end{pmatrix},$$

$$S = \frac{e^{i\varphi_s}}{\sqrt{2}}(v_s + h_s + i a_s) \,, \tag{6}$$

with the CP-violating phases $\varphi_{u,s}$. After EWSB, the W and Z bosons get masses,

$$M_W^2 = \frac{1}{4} g_2^2 \left(v_u^2 + v_d^2\right) \,, \quad M_Z^2 = \frac{1}{4}(g_1^2 + g_2^2)\left(v_u^2 + v_d^2\right). \tag{7}$$

The two VEVs v_u and v_d are replaced by $\tan\beta$ and the SM VEV,

$$\tan\beta = \frac{v_u}{v_d}, \quad v^2 = v_u^2 + v_d^2 \,, \tag{8}$$

and the singlet VEV is related to the effective μ parameter by

$$\mu_{\text{eff}} = \frac{\lambda v_s e^{i\varphi_s}}{\sqrt{2}}. \tag{9}$$

The Higgs potential can be cast into the form

$$\begin{aligned} V_H = &\, V_H^{\text{const}} + t_{h_d} h_d + t_{h_u} h_u + t_{h_s} h_s + t_{a_d} a_d + t_{a_u} a_u + t_{a_s} a_s \\ &+ \frac{1}{2} \phi^{0,T} \mathcal{M}_{\phi\phi}\, \phi^0 + \phi^{c,\dagger} \mathcal{M}_{h^+h^-}\, \phi^c + V_H^{\phi^3} + V_H^{\phi^4}, \end{aligned} \tag{10}$$

with $\phi^0 \equiv (h_d, h_u, h_s, a_d, a_u, a_s)^T$ and $\phi^c \equiv ((h_d^-)^*, h_u^+)^T$. The six tadpole coefficients are given by

$$\begin{aligned} \frac{t_{h_d}}{v_d} = &\, m_{H_d}^2 + \frac{c_{2\beta} M_Z^2}{2} - \frac{|\lambda| \tan\beta\, v_s}{2} \Big(|\kappa| c_{\varphi_y} v_s \\ &- \sqrt{2}\text{Im} A_\lambda s_{\varphi_\omega - \varphi_y} + \sqrt{2}\text{Re} A_\lambda c_{\varphi_\omega - \varphi_y}\Big) \\ &+ \frac{1}{2}|\lambda|^2 \left(s_\beta{}^2 v^2 + v_s^2\right) \end{aligned} \tag{11a}$$

$$\begin{aligned} \frac{t_{h_u}}{v_u} = &\, m_{H_u}^2 - \frac{c_{2\beta} M_Z^2}{2} - \frac{|\lambda| v_s}{2\tan\beta} \Big(|\kappa| c_{\varphi_y} v_s - \sqrt{2}\text{Im} A_\lambda s_{\varphi_\omega - \varphi_y} \\ &+ \sqrt{2}\text{Re} A_\lambda c_{\varphi_\omega - \varphi_y}\Big) \\ &+ \frac{1}{2}|\lambda|^2 \left(c_\beta{}^2 v^2 + v_s^2\right) \end{aligned} \tag{11b}$$

$$\begin{aligned} \frac{t_{h_s}}{v_S} = &\, m_S^2 + |\kappa|^2 v_s^2 + \frac{|\lambda|^2 v^2}{2} + |\lambda| c_\beta s_\beta v^2 \\ &\left(\frac{\text{Im} A_\lambda s_{\varphi_\omega - \varphi_y} - \text{Re} A_\lambda c_{\varphi_\omega - \varphi_y}}{\sqrt{2} v_s} - |\kappa| c_{\varphi_y}\right) \\ &+ \frac{|\kappa| v_s (\text{Re} A_\kappa c_{\varphi_\omega} - \text{Im} A_\kappa s_{\varphi_\omega})}{\sqrt{2}} \end{aligned} \tag{11c}$$

$$\begin{aligned} \frac{t_{a_d}}{v_d} = &\, \frac{1}{2}|\lambda| v_s \Big(-|\kappa| v_s s_{\varphi_y} + \sqrt{2}\text{Im} A_\lambda c_{\varphi_\omega - \varphi_y} \\ &+ \sqrt{2}\text{Re} A_\lambda s_{\varphi_\omega - \varphi_y}\Big) \end{aligned} \tag{11d}$$

$$t_{a_u} = \frac{1}{\tan\beta} t_{a_d} \tag{11e}$$

$$t_{a_s} = \frac{1}{2}|\lambda| c_\beta s_\beta v^2 \left(2|\kappa| v_s s_{\varphi_y} + \sqrt{2}\mathrm{Im}A_\lambda c_{\varphi_\omega - \varphi_y} + \sqrt{2}\mathrm{Re}A_\lambda s_{\varphi_\omega - \varphi_y}\right) - \frac{|\kappa| v_s^2 (\mathrm{Im}A_\kappa c_{\varphi_\omega} + \mathrm{Re}A_\kappa s_{\varphi_\omega})}{\sqrt{2}} , \tag{11f}$$

where the complex parameters A_λ and A_κ are decomposed into the corresponding imaginary and real parts. We introduced the short-hand notation $c_x \equiv \cos x$ and $s_x \equiv \sin x$. The two combinations of phases that enter the tree-level potential are

$$\varphi_y = \varphi_\kappa - \varphi_\lambda + 2\varphi_s - \varphi_u \tag{12a}$$

$$\varphi_\omega = \varphi_\kappa + 3\varphi_s \, . \tag{12b}$$

Since we require the five independent tadpoles to vanish at the minimum of the potential, we can use these minimum conditions to eliminate a set of five parameters which we choose as $\{m^2_{H_d}, m^2_{H_u}, m^2_S, \mathrm{Im}A_\lambda, \mathrm{Im}A_\kappa\}$. The 6×6 mass matrix for the neutral Higgs bosons, $\mathcal{M}_{\phi\phi}$, and the 2×2 mass matrix for the charged Higgs bosons, $\mathcal{M}_{h^+h^-}$, can be found in [104]. The triple Higgs interactions are collected in $V_H^{\phi^3}$, their explicit expressions can be found in the appendix A of [76]. Constant terms and quartic interactions are summarized in V_H^{const} and $V_H^{\phi^4}$, respectively.

The neutral Higgs mass matrix $\mathcal{M}_{\phi\phi}$ is diagonalized by an orthogonal matrix $\mathcal{R}^H$ such that

$$\mathrm{diag}(m^2_{h_1}, m^2_{h_2}, m^2_{h_3}, m^2_{h_4}, m^2_{h_5}, M^2_{G^0}) = \mathcal{R}^H \mathcal{M}_{\phi\phi} \mathcal{R}^{H,T}, \tag{13a}$$

$$(h_1, h_2, h_3, h_4, h_5, G^0)^T = \mathcal{R}^H (h_d, h_u, h_s, a_d, a_u, a_s)^T . \tag{13b}$$

The tree-level masses are in ascending order, $m_{h_1} \leq m_{h_2} \leq m_{h_3} \leq m_{h_4} \leq m_{h_5}$. In the 't Hooft–Feynman gauge, the neutral Goldstone boson tree-level mass is equal to the Z boson tree-level mass. The charged Higgs mass matrix $\mathcal{M}_{h^+h^-}$ is diagonalized with an orthogonal matrix $\mathcal{R}^{H^\pm}$,

$$\mathrm{diag}(M^2_{H^\pm}, M^2_{G^\pm}) = \mathcal{R}^{H^\pm} \mathcal{M}_{h^+h^-} (\mathcal{R}^{H^\pm})^T , \tag{14a}$$

$$\mathcal{R}^{H^\pm} = \begin{pmatrix} -\cos\beta & \sin\beta \\ \sin\beta & \cos\beta \end{pmatrix} , \tag{14b}$$

where the charged Goldstone boson tree-level mass is equal to the W boson tree-level mass in the 't Hooft-Feynman gauge.

We chose the set of independent parameters entering the Higgs potential as

$$\{t_{h_d}, t_{h_u}, t_{h_s}, t_{a_d}, t_{a_s}, M_{H^\pm}, M_W, M_Z, e, \tan\beta, |\lambda|, \mu_{\text{eff}}, |\kappa|, \mathrm{Re}A_\kappa, \varphi_\lambda, \varphi_\kappa, \varphi_u, \varphi_s\} , \tag{15}$$

or alternatively with $\mathrm{Re}A_\lambda$ instead of the charged Higgs mass as input

$$\{t_{h_d}, t_{h_u}, t_{h_s}, t_{a_d}, t_{a_s}, M_W, M_Z, e, \tan\beta, |\lambda|, \mu_{\text{eff}}, |\kappa|, \mathrm{Re}A_\lambda, \mathrm{Re}A_\kappa, \varphi_\lambda, \varphi_\kappa, \varphi_u, \varphi_s\} . \tag{16}$$

The gauge, quark and charged lepton sectors of the NMSSM-nuSS are similar to the SM. Likewise, the neutralino, chargino, up squark, down squark, charged slepton sectors are similar to the ones of the complex NMSSM. We review here the neutrino and sneutrino sectors which we focus on in this study. With the NMSSM-nuSS superpotential in Eq. (1), one can derive the mass matrix describing the mixing between the three left-handed neutrino components, ν_L, with the fermionic fields of the six leptonic singlet superfields, $\hat{N}^c_i$, $\hat{X}_i$, $i = 1, 2, 3$,

$$\mathcal{L}^\nu_{\text{mass}} = -\frac{1}{2} \begin{pmatrix} \nu_L & N^c & X \end{pmatrix} M^\nu_{\text{ISS}} \begin{pmatrix} \nu_L \\ N^c \\ X \end{pmatrix} , \tag{17}$$

where ν_L, N^c and X are left-handed Weyl spinors and

$$M^\nu_{\text{ISS}} = \begin{pmatrix} 0 & M_D & 0 \\ M_D^T & 0 & M_X \\ 0 & M_X^T & \mu_X \end{pmatrix} . \tag{18}$$

The mass blocks M_D, M_X and μ_X are 3×3 matrices and

$$M_D = \frac{v_u e^{i\varphi_u}}{\sqrt{2}} y_\nu \, , \quad \mu_X = \frac{v_s e^{i\varphi_s}}{\sqrt{2}} (\lambda_X + \lambda_X^T) \, . \tag{19}$$

In the inverse seesaw mechanism, one assumes that there is a hierarchy in the eigenvalues of the matrices μ_X, M_D and M_X, $|m^{\mu_X}| \ll |m^{M_D}| \ll |m^{M_X}|$, so that neutrino masses around eV can be obtained with M_X elements of $\mathcal{O}$(TeV) and $y_\nu \sim \mathcal{O}(1)$. With this mass hierarchy, the 3×3 light neutrino mass matrix can be approximated at leading order as

$$M_{\text{light}} = M_D M_N^{-1} M_D^T \, , \quad \text{with} \quad M_N = M_X \mu_X^{-1} M_X^T \, , \tag{20}$$

and is diagonalized by the Pontecorvo–Maki–Nakagawa–Sakata (PMNS) matrix U_{PMNS},

$$U^*_{\text{PMNS}} M_{\text{light}} U^\dagger_{\text{PMNS}} = m_\nu , \quad m_\nu = \mathrm{diag}(m_{\nu_1}, m_{\nu_2}, m_{\nu_3}) . \tag{21}$$

Neutrino oscillation data constrain the neutrino masses (or relations among them) and the mixing angles entering U_{PMNS}. In order to be able to use these experimental results as input, we re-parameterize the neutrino sector accordingly. There are two common parameterizations in the literature. Both parametrizations make use of Eq. (21) such that the

light neutrino oscillation data can be taken as input parameters. The three complex matrices M_D, μ_X, M_X are then not entirely independent, but one of them will be computed from the others. In the Casas-Ibarra parameterization [105], M_D is computed from the relation

$$\begin{aligned} M_D &= U_{\text{PMNS}}^T \sqrt{m_\nu} R \sqrt{\mathcal{M}_N} V_\nu, \\ \mathcal{M}_N &= \text{diag}(M_{N_1}, M_{N_2}, M_{N_3}) = V_\nu^* M_N V_\nu^\dagger, \end{aligned} \tag{22}$$

with R being a complex orthogonal matrix parameterized by three complex angles $(\tilde{\theta}_{1,2,3})$, and V_ν is a unitary matrix diagonalizing M_N. One can then obtain y_ν from Eq. (19). In this parameterization, the set of input parameters in the neutrino sector reads

$$m_{\nu_1}, m_{\nu_2}, m_{\nu_3}, \theta_{12}, \theta_{23}, \theta_{13}, \delta_{CP}, \tilde{\theta}_1, \tilde{\theta}_2, \tilde{\theta}_3, M_X, \mu_X. \tag{23}$$

The second possibility used in this work is the μ_X-parameterization [106] in which μ_X is computed from the relation derived from Eqs. (20) and (21),

$$\mu_X = M_X^T M_D^{-1} U_{\text{PMNS}}^* m_\nu U_{\text{PMNS}}^\dagger M_D^{T,-1} M_X, \tag{24}$$

where M_D is calculated from the input y_ν. Therefore the set of input parameters in this parameterization is given by

$$m_{\nu_1}, m_{\nu_2}, m_{\nu_3}, \theta_{12}, \theta_{23}, \theta_{13}, \delta_{CP}, M_X, y_\nu. \tag{25}$$

After using one of the two parameterizations, we have fixed all degrees of freedom of the three complex matrices M_D, μ_X, M_X. We diagonalize the 9×9 neutrino mass matrix in Eq. (18) numerically using quadruple precision to obtain a unitary rotation matrix U^ν and nine neutrino mass eigenstates with their masses m_{n_i} $(i = 1, ..., 9)$ being sorted in ascending order,

$$\mathcal{U}_\nu^* M_{\text{ISS}}^\nu \mathcal{U}_\nu^\dagger = \text{diag}(m_{n_1}, \ldots, m_{n_9}). \tag{26}$$

We define the Majorana neutrino fields as

$$\begin{aligned} n_i = \begin{pmatrix} \nu_i \\ \overline{\nu_i} \end{pmatrix} \quad \text{with} \quad \nu_i &= (\mathcal{U}_\nu)_{ik} \nu_{L,k} + (\mathcal{U}_\nu)_{i(k+3)} N_k^c \\ &+ (\mathcal{U}_\nu)_{i(k+6)} X_k, \end{aligned} \tag{27}$$

where $i = 1, ..., 9$, $k = 1, 2, 3$, and

$$\overline{\nu_i} = i\sigma_2 \nu_i^*. \tag{28}$$

The Majorana neutrino fields, n_i, and their corresponding mass eigenvalues are then used in our actual computation.

In the sneutrino sectors, we decompose each complex scalar field into its CP-even and CP-odd components,

$$\tilde{\nu} = \frac{1}{\sqrt{2}} (\tilde{\nu}_+ + i\tilde{\nu}_-) , \tag{29a}$$

$$\tilde{N}^* = \frac{1}{\sqrt{2}} \left(\tilde{N}_+ + i\tilde{N}_- \right) , \tag{29b}$$

$$\tilde{X} = \frac{1}{\sqrt{2}} \left(\tilde{X}_+ + i\tilde{X}_- \right) . \tag{29c}$$

Due to non-vanishing CP-violating phases, the 9 CP-even components mix with the 9 CP-odd ones resulting in the mass term in the Lagrangian

$$\mathcal{L}_{\tilde{\nu}} = \frac{1}{2} \psi^T M_{\tilde{\nu}} \psi , \tag{30}$$

where $\psi = (\tilde{\nu}_+, \tilde{N}_+, \tilde{X}_+, \tilde{\nu}_-, \tilde{N}_-, \tilde{X}_-)^T$ and $M_{\tilde{\nu}}$ is an 18×18 symmetric matrix which can be found in [51]. We then diagonalize the mass matrix $M_{\tilde{\nu}}$ with an orthogonal matrix $\mathcal{U}_{\tilde{\nu}}$

$$\text{diag}\left(m_{\tilde{n}_1}^2, \ldots, m_{\tilde{n}_{18}}^2 \right) = \mathcal{U}_{\tilde{\nu}} M_{\tilde{\nu}} \mathcal{U}_{\tilde{\nu}}^T , \tag{31}$$

and order the mass values as $m_{\tilde{n}_1}^2 \leq \cdots \leq m_{\tilde{n}_{18}}^2$. In addition to parameters in the neutrino sector, the sneutrino sector has the following chosen input parameters

$$A_\nu, m_{\tilde{L}}, m_{\tilde{X}}, m_{\tilde{N}}, B_{\mu_X}, \tag{32}$$

which are used to numerically obtain the mass eigenvalues and mixing matrices as described above.

3 Loop corrections to the effective THCs and Higgs-to-Higgs decays

Loop corrections are important for both the Higgs mass predictions and the triple Higgs couplings. In order to investigate a correlation between the two quantities, it is therefore mandatory to perform the calculation of the two using the same framework, *e.g.* renormalization schemes and approximations. In this model, there are five neutral Higgs bosons, many of the triple Higgs couplings are non-vanishing at the tree-level. We consider the loop-corrections to all of them, therefore, the loop-corrected THCs considered in this study can be expressed as follows:

$$\begin{aligned} \hat{\lambda}_{h_i h_j h_k} = \lambda_{h_i h_j h_k} + \Delta\lambda^{(1)}_{h_i h_j h_k} + \Delta\lambda^{(2,\alpha_s\alpha_t)}_{h_i h_j h_k} + \Delta\lambda^{(2,\alpha_t^2)}_{h_i h_j h_k}, \\ i, j, k = 1, ..., 5, \end{aligned} \tag{33}$$

where $\lambda_{h_i h_j h_k}$ are the tree-level THCs, $\Delta\lambda^{(1)}_{h_i h_j h_k}$ denotes the one-loop corrections and $\Delta\lambda^{(2,\alpha_s\alpha_t)}_{h_i h_j h_k}$, $\Delta\lambda^{(2,\alpha_t^2)}_{h_i h_j h_k}$ are the dominant two-loop QCD and electroweak corrections, respectively. These two-loop corrections have been previously computed in the zero momentum approximation in [76,77] for the CP-violating NMSSM without inverse seesaw mechanism. However, it is possible to embed them into the NMSSM-nuSS in a straight-forward way [51]. Therefore, the approximation in the THCs is the same as the one in the Higgs mass

calculation which includes also the two-loop $\mathcal{O}(\alpha_s\alpha_t)$ and $\mathcal{O}(\alpha_t^2)$ corrections.

In general, these loop-corrected THCs depend on the external momenta. If the decay of the heavier Higgs bosons into two lighter Higgs bosons is kinematically allowed, we compute the decay width using the loop-corrected THCs and the on-shell (OS) condition for external Higgs bosons. This means that we set the momentum squared for each external leg equal to the loop-corrected Higgs mass squared. To ensure that the OS condition of the external Higgs bosons is fulfilled, we take into account the appropriate wave-function renormalization (WFR) factors [75,78]. The partial decay width for the decay channel $H_i \to H_j H_k$, where capital H denotes the loop-corrected mass eigenstates and small h the tree-level mass eigenstates, is then given by

$$\Gamma_{H_i\to H_jH_k} = R_2 \frac{\lambda^{1/2}(M_{H_i}^2, M_{H_j}^2, M_{H_k}^2)}{16\pi M_{H_i}^3} \times \left| \sum_{i_1,j_1,k_1=1}^{5} \mathbf{Z}^H_{ii_1}\mathbf{Z}^H_{jj_1}\mathbf{Z}^H_{kk_1}\hat{\lambda}_{h_ih_jh_k}(M_{H_i}^2, M_{H_j}^2, M_{H_k}^2)\right|^2 . \tag{34}$$

Here $R_2 = 1/2$ for two identical final states and $R_2 = 1$ otherwise. $\mathbf{Z}$ denotes the wave-function renormalization factor, which can be found in [75] for the real case and in [78] for the complex case. In the following, we use M_{H_i} $(i = 1, ..., 5)$ to denote the loop-corrected Higgs masses and m_{h_i} to denote the tree-level ones. All possible decay channels have been integrated into the computation of the total decay widths and decay branching ratios of the heavy Higgs boson states.

The trilinear Higgs self-couplings are not only important for Higgs decays, but can also enter e.g. the prediction for Higgs pair production. At the LHC the dominant Higgs pair production process is given by gluon fusion into Higgs pairs which is a loop induced process. We discuss here only the gluon fusion into two SM-like Higgs bosons, $gg \to H_iH_i$ ($H_i \equiv H_{\rm SM}$). At leading order, the Feynman diagrams, involving triangle and box contributions, are similar to the MSSM case [107,108], except for the ones involving a scalar Higgs boson in the s-channel, which gets contributions from five neutral NMSSM Higgs bosons in the general CP-violating case. Thus the cross section involves couplings of the form $\lambda_{H_{\rm SM}H_{\rm SM}H_{\rm SM}}$ and $\lambda_{H_{\rm SM}H_{\rm SM}H_k\neq H_{\rm SM}}$. Assuming that the loop corrections to the gluon fusion process are dominated by the corrections to the trilinear Higgs self-couplings, which is the case for large corrections to the couplings between the Higgs bosons, the loop-corrected trilinear Higgs self-couplings can be used in the leading-order gluon fusion process in order to obtain an approximate loop-corrected production cross section. A proper treatment would require the inclusion of the momentum dependence in the trilinear Higgs self-coupling as well as the calculation of notoriously difficult massive double-box diagrams. This is beyond the purpose of the analysis in this paper, where we only want to investigate the effects of the extended (s)neutrino sectors on the $gg \to H_{\rm SM}H_{\rm SM}$ process.[3] Therefore, we simplify our investigation by using the effective loop-corrected THCs, which are computed at zero external momenta. For this, we include the effective loop-corrected THCs that contain the dominant one- and two-loop contributions arising from the (s)top sector as in Eq. (33) and the one-loop contributions from the extended (s)neutrino sector. In the following, we describe in detail our computation of the complete one-loop contribution in the NMSSM-nuSS to the triple Higgs couplings including the full momentum dependence $\hat{\lambda}^{(1)}_{h_ih_jh_k}(p_1^2, p_2^2, p_3^2)$ and subsequently introduce the effective trilinear Higgs self-couplings.

3.1 Complete one-loop corrections with full momentum dependence

The renormalized one-loop corrections to the THCs can be written in terms of the unrenormalized one-loop contribution $\lambda^{(1)}_{h_ih_jh_k}$ and the counterterm $\delta\lambda^{(1)}_{h_ih_jh_k}$,

$$\Delta\lambda^{(1)}_{h_ih_jh_k}(p_1^2, p_2^2, p_3^2) = \lambda^{(1)}_{h_ih_jh_k}(p_1^2, p_2^2, p_3^2) + \delta\lambda^{(1)}_{h_ih_jh_k}, \tag{35}$$

where the $\lambda^{(1)}_{h_ih_jh_k}$ are computed from genuine one-loop triangle diagrams generated with `FeynArts-3.11` [110,111] and processed with `FormCalc-9.8` [112] including full external momentum dependence. The one-loop counterterms can be written as

$$\delta\lambda^{(1)}_{h_ih_jh_k} = \frac{1}{2}\sum_{l=1}^{6}\Big(\delta Z_{h_ih_l}\lambda_{h_lh_jh_k} + \delta Z_{h_jh_l}\lambda_{h_ih_lh_k} + \delta Z_{h_kh_l}\lambda_{h_ih_jh_l}\Big) + \sum_{i_1,j_1,k_1=1}^{6}\mathcal{R}^H_{ii_1}\mathcal{R}^H_{jj_1}\mathcal{R}^H_{kk_1}\delta\lambda^{hhh}_{i_1j_1k_1}, \tag{36}$$

where we have identified $h_6 \equiv G^0$ for simplicity of notation, $\mathcal{R}^H$ is the Higgs rotation matrix defined in Eq. (13b) and $\delta\lambda^{hhh}_{i_1j_1k_2}$ are the counterterms in the interaction eigenstates $(h_d, h_u, h_s, a_d, a_u, a_s)$ and are given in appendix C of [76].

The renormalization scheme applied in this calculation is the mixed OS-$\overline{\rm DR}$ scheme as in our Higgs mass calculation [51]. Here, we have the following two options. In the first

[3] For a discussion of the momentum effects cf. e.g. [90,109].

option, the input parameters are renormalized as

$$\begin{aligned}&\underbrace{t_{h_d}, t_{h_u}, t_{h_s}, t_{a_d}, t_{a_s}, M_{H^\pm}, M_W, M_Z, e}_{\text{OS}},\\&\underbrace{\tan\beta, |\lambda|, |\mu_{\text{eff}}|, |\kappa|, \text{Re}A_\kappa}_{\overline{\text{DR}}},\end{aligned} \tag{37}$$

where the first nine parameters including five tadpoles, three masses and the electric coupling are renormalized in the OS scheme, and the last five parameters are renormalized in the $\overline{\text{DR}}$ scheme. The complex phases $\varphi_\lambda, \varphi_\kappa, \varphi_u, \varphi_s$ do not get counterterms at the one-loop order. The explicit renormalization conditions for these parameters can be found in [51]. In the second option, with $\text{Re}(A_\lambda)$ as input parameter instead of $M_{H^\pm}$, we renormalize the input parameters according to

$$\begin{aligned}&\underbrace{t_{h_d}, t_{h_u}, t_{h_s}, t_{a_d}, t_{a_s}, M_W, M_Z, e}_{\text{OS}},\\&\underbrace{\tan\beta, |\lambda|, \mu_{\text{eff}}, |\kappa|, \text{Re}A_\lambda, \text{Re}A_\kappa}_{\overline{\text{DR}}}.\end{aligned} \tag{38}$$

We have checked that $\Delta\lambda^{(1)}_{h_i h_j h_k}(p_1^2, p_2^2, p_3^2)$ are UV finite and that in the limit of vanishing neutrino Yukawa couplings, our results are in agreement with [75] for the real NMSSM and with [76] for the complex NMSSM.

3.2 Dominant one-loop corrections to the effective THCs

The effective loop-corrected THCs can be defined as the third derivative of the effective potential with respect to the Higgs fields as

$$\hat{\lambda}^{\text{eff}}_{h_i h_j h_k} = \frac{\partial^2 V_H^{\text{eff}}}{\partial h_i \partial h_j \partial h_k}, \tag{39}$$

which is equivalent to $\hat{\lambda}_{h_i h_j h_k}$ in Eq. (33) evaluated at zero external momenta. However, the zero-external-momentum approximation is known to become unreliable in scenarios that feature very light or even mass-less scalar states. The singlet-like pseudoscalar state of the NMSSM is a possible candidate for such a state [75]. Therefore, it is important to organize the calculation to be numerically robust in scenarios with a light pseudoscalar. While several workarounds exist in the literature, see e.g. Refs. [113–117], we simply evade the problem of infra-red divergences by identifying the dominant contributions to the effective trilinear coupling and compute them explicitly at vanishing external momenta. Therefore, all two-point and three-point one-loop integrals will be written in terms of one-loop tadpole integrals. We compute the effective trilinear couplings assuming that the most dominant contributions are the $\mathcal{O}(\alpha_t)$ corrections originating from the (s)top sector, due to the large top Yukawa coupling, and the (s)neutrino contributions that also naturally feature O(1) Yukawa couplings due to the inverse seesaw mechanism. To further simplify the calculation and to focus on the largest corrections, we have performed the calculation in the gaugeless limit where the electric coupling is set to zero ($e \to 0$) but the electroweak VEV is kept non-zero ($v \neq 0$). For the $\mathcal{O}(\alpha_t)$ corrections, the following set of parameters has to be renormalized,

$$t_{h_d}, t_{h_u}, t_{h_s}, t_{a_d}, t_{a_s}, M^2_{H^\pm}, v, \tan\beta, |\lambda|, \tag{40}$$

where the first seven parameters are renormalized in the OS scheme and the last two parameters are renormalized in the $\overline{\text{DR}}$ scheme. Explicit expressions of the $\mathcal{O}(\alpha_t)$ contributions to the one-loop counterterms, $\delta t_{h_d}, \delta t_{h_u}, \delta t_{h_s}, \delta t_{a_d}, \delta t_{a_s}$, $\delta M^2_{H^\pm}, \delta v, \delta\tan\beta, \delta|\lambda|$, are given in [76]. In this study we assume that the neutrino Yukawa couplings are large. Therefore, the contributions from the (s)neutrino sector can be significant. In the following, we present the analytic expressions of the neutrino and sneutrino contributions for the OS counterterms ($\delta t_{h_d}, \delta t_{h_u}, \delta t_{h_s}, \delta t_{a_d}, \delta t_{a_s}, \delta M^2_{H^\pm}, \delta v$). In the gaugeless limit, the counterterm of the SM VEV can be expressed as

$$\frac{\delta v}{v} = \frac{c_W^2}{2s_W^2}\left(\frac{\delta M_Z^2}{M_Z^2} - \frac{\delta M_W^2}{M_W^2}\right) + \frac{1}{2}\frac{\delta M_W^2}{M_W^2}, \tag{41}$$

where

$$\begin{aligned}\frac{\delta M_W^2}{M_W^2} =& -\sum_{i=1}^{9}\frac{m^2_{n_i}\sum_{j=1}^{3}|\mathcal{U}_{\nu_{ij}}|^2}{8\pi^2 v^2}\frac{1}{\epsilon}\\&+\frac{1}{32\pi^2 v^2}\Bigg[\sum_{i=1}^{3}\sum_{j=1}^{18}(\mathcal{U}^2_{\tilde{n}_{ji}} + \mathcal{U}^2_{\tilde{\nu}_{j(i+9)}})F_0(m^2_{\tilde{n}_j}, m^2_{\tilde{L}_i})\end{aligned} \tag{42}$$

$$\begin{aligned}&+4\sum_{i=1}^{3}A_0(m^2_{\tilde{L}_i}) - 2\sum_{i=1}^{9}\left(1 - 2\ln\overline{m^2_{n_i}}\right))\\&m^2_{n_i}\sum_{j=1}^{3}|\mathcal{U}_{\nu_{ij}}|^2\Bigg]\end{aligned} \tag{43}$$

$$\begin{aligned}\frac{\delta M_Z^2}{M_Z^2} =& -\sum_{i=1}^{9}\frac{m^2_{n_i}\sum_{j=1}^{3}|\mathcal{U}_{\nu_{ij}}|^2}{8\pi^2 v^2}\frac{1}{\epsilon}\\&+\frac{1}{8\pi^2 v^2}\Bigg[\sum_{i=1}^{18}g_{\tilde{\nu}_i\tilde{\nu}_i ZZ}A_0(m^2_{\tilde{n}_i})\\&+4\sum_{i,j=1}^{18}g^2_{\tilde{\nu}_i\tilde{\nu}_j Z}B_{00}(m^2_{\tilde{n}_i}, m^2_{\tilde{n}_j})\Bigg]\\&+2\sum_{i,j=1}^{9}\Bigg[-2B_0(m^2_{n_i}, m^2_{n_j})(|g^L_{\nu_i\nu_j z}|^2 + i \leftrightarrow j)\end{aligned}$$

$$-4(A_0(m^2_{n_j}) - 2B_{00}(m^2_{n_i}, m^2_{n_j}) + B_0(m^2_{n_i}, m^2_{n_j})m^2_{n_i})|g^L_{\nu_i\nu_j z}|^2\Big] \quad (44)$$

where $\ln\overline{m^2_{n_i}} = \ln(m^2_{n_i}/\mu^2_R)$ (μ_R denotes the renormalization scale) and the couplings read

$$g_{\tilde{\nu}_i\tilde{\nu}_j ZZ} = \frac{1}{2}\sum_{k=1}^{3}\left(\mathcal{U}^*_{\tilde{\nu}_{ik}}\mathcal{U}^*_{\tilde{\nu}_{jk}} + \mathcal{U}^*_{\tilde{\nu}_{i(k+9)}}\mathcal{U}^*_{\tilde{\nu}_{j(k+9)}}\right), \quad (45)$$

$$g_{\tilde{\nu}_i\tilde{\nu}_j Z} = \frac{1}{2}\sum_{k=1}^{3}\left(\mathcal{U}^*_{\tilde{\nu}_{i(k+9)}}\mathcal{U}^*_{\tilde{\nu}_{jk}} - \mathcal{U}^*_{\tilde{\nu}_{ik}}\mathcal{U}^*_{\tilde{\nu}_{j(k+9)}}\right), \quad (46)$$

$$g^L_{\nu_i\nu_j Z} = \frac{1}{2}\sum_{k=1}^{3}\mathcal{U}_{\nu_{ik}}\mathcal{U}^*_{\nu_{jk}}. \quad (47)$$

The charged Higgs mass counterterm is given by

$$\begin{aligned}\delta M^2_{H^\pm} = &-\frac{1}{32\pi^2}g_{H^+\tilde{n}_i\tilde{n}_i H^-}A^\epsilon_0(m^2_{\tilde{n}_i}) \\ &-\frac{1}{16\pi^2}g_{H^+\tilde{l}_i\tilde{l}_i H^-}A^\epsilon_0(m^2_{\tilde{l}_i}) \\ &+\frac{1}{16\pi^2}\left|g_{\tilde{n}_i\tilde{l}_j H^-}\right|^2 B^\epsilon_0(m^2_{\tilde{l}_j}, m^2_{\tilde{n}_i}) \\ &-\frac{1}{8\pi^2}m^2_{n_i}\left|g^L_{n_i l_j H^+}\right|^2 B^\epsilon_0(0, m^2_{n_i}),\end{aligned} \quad (48)$$

and the neutral Higgs tadpole counterterms t_{h_α} ($h_\alpha = h_d, h_u, h_s, a_d, a_s$) read

$$\begin{aligned}\delta^{(1)}t_{h_\alpha} = &-\sum_{j=1}^{18}\frac{g_{h_i\tilde{n}_j\tilde{n}_j}}{32\pi^2}A^\epsilon_0(m^2_{\tilde{n}_j}) \\ &+\frac{1}{8\pi^2}\mathrm{Re}[g^L_{h_i n_j n_j}]m_{n_j}A^\epsilon_0(m^2_{n_j}).\end{aligned} \quad (49)$$

The couplings of the charged Higgs boson to the neutrinos, the charged leptons, the sneutrinos and the selectrons are given by

$$\begin{aligned}g_{H^+\tilde{n}_i\tilde{n}_j H^-} = &-\frac{1}{2}c^2_\beta\sum_{l_1,l_2,l_3}^{3}(y_\nu)_{l_1,l_2}(y_\nu)^*_{l_1,l_3} \\ &\times\Big[\mathcal{U}^{\tilde{\nu}}_{i,l_3+3}\left(\mathcal{U}^{\tilde{\nu}}_{j,l_2+3} - i\,\mathcal{U}^{\tilde{\nu}}_{j,l_2+12}\right) \\ &+\mathcal{U}^{\tilde{\nu}}_{i,l_3+12}\left(\mathcal{U}^{\tilde{\nu}}_{j,l_2+12} + i\,\mathcal{U}^{\tilde{\nu}}_{j,l_2+3}\right) \\ &+\left(\mathcal{U}^{\tilde{\nu}}_{i,l_2+3} - i\,\mathcal{U}^{\tilde{\nu}}_{i,l_2+12}\right)\left(\mathcal{U}^{\tilde{\nu}}_{j,l_3+3} + i\,\mathcal{U}^{\tilde{\nu}}_{j,l_3+12}\right)\Big] \\ &+\frac{1}{2}c_\beta\, s_\beta\sum_{l_2,l_1}^{3}\Big\{e^{i\varphi_u}\lambda(\lambda_X{}^*)_{l_2,l_1} \\ &\times\Big[-\mathcal{U}^{\tilde{\nu}}_{i,l_2+6}\left(\mathcal{U}^{\tilde{\nu}}_{j,l_1+6} - i\,\mathcal{U}^{\tilde{\nu}}_{j,l_1+15}\right) \\ &+\mathcal{U}^{\tilde{\nu}}_{i,l_2+15}\left(\mathcal{U}^{\tilde{\nu}}_{j,l_1+15} + i\,\mathcal{U}^{\tilde{\nu}}_{j,l_1+6}\right) \\ &-\left(\mathcal{U}^{\tilde{\nu}}_{i,l_1+6} - i\,\mathcal{U}^{\tilde{\nu}}_{i,l_1+15}\right) \\ &\left(\mathcal{U}^{\tilde{\nu}}_{j,l_2+6} - i\,\mathcal{U}^{\tilde{\nu}}_{j,l_2+15}\right)\Big] - e^{-i\varphi_u}\lambda^c\,(\lambda_X)_{l_2,l_1} \\ &\times\Big[\mathcal{U}^{\tilde{\nu}}_{i,l_2+6}\left(\mathcal{U}^{\tilde{\nu}}_{j,l_1+6} + i\mathcal{U}^{\tilde{\nu}}_{j,l_1+15}\right) \\ &+i\,\mathcal{U}^{\tilde{\nu}}_{i,l_2+15}\left(\mathcal{U}^{\tilde{\nu}}_{j,l_1+6} + i\,\mathcal{U}^{\tilde{\nu}}_{j,l_1+15}\right) \\ &+\left(\mathcal{U}^{\tilde{\nu}}_{i,l_1+6} + i\,\mathcal{U}^{\tilde{\nu}}_{i,l_1+15}\right) \\ &\left(\mathcal{U}^{\tilde{\nu}}_{j,l_2+6} + i\,\mathcal{U}^{\tilde{\nu}}_{j,l_2+15}\right)\Big]\Big\},\end{aligned} \quad (50)$$

$$\begin{aligned}g_{\tilde{n}_i\tilde{l}_j H^-} = &\,c_\beta\sum_{l_1,l_2,l_3}^{3}\Big\{\frac{1}{\sqrt{2}}e^{-i\varphi_u}\,(\mu_X)_{l_1,l_2}\delta_{j,l_3} \\ &\left(\mathcal{U}^{\tilde{\nu}}{}_{i,l_2+6} + i\mathcal{U}^{\tilde{\nu}}_{i,l_2+15}\right) \\ &(y_\nu)^*_{l_3,l_1} + \frac{1}{2}v_u(y_\nu)^*_{l_3,l_1}\delta_{j,l_3}(y_\nu)_{l_2,l_1} \\ &\left(\mathcal{U}^{\tilde{\nu}*}_{i,l_2} + i\mathcal{U}^{\tilde{\nu}}_{i,l_2+9}\right)\Big\} \\ &+\sum_{l_2,l_1}^{3}\Big\{\frac{1}{\sqrt{2}}c_\beta e^{-i\varphi_u}\,\delta_{j,l_1}(y_\nu A_\nu)_{l_1,l_2} \\ &\left(\mathcal{U}^{\tilde{\nu}}_{i,l_2+3} + i\mathcal{U}^{\tilde{\nu}}{}_{i,l_2+12}\right) \\ &+\frac{1}{2}\lambda s_\beta v_S(y^*_\nu)_{l_1,l_2}e^{i\varphi_s}\delta_{j,l_1}\left(\mathcal{U}^{\tilde{\nu}}_{i,l_2+3} + i\mathcal{U}^{\tilde{\nu}}_{i,l_2+12}\right)\Big\},\end{aligned} \quad (51)$$

$$g_{H^+\tilde{l}_i\tilde{l}_j H^-} = -c^2_\beta\sum_{l_1,l_2,l_3}^{3}\delta_{j,l_3}\delta_{i,l_2}(y_\nu)_{l_2,l_1}\,(y^*_\nu)_{l_3,l_1}, \quad (52)$$

$$g^L_{n_i l_j H^+} = c_\beta\sum_{l_2,l_1}^{3}e^{i\varphi_u}(y_\nu)_{l_1,l_2}\,\delta_{j,l_1}\mathcal{U}^\nu_{i,l_2+3}. \quad (53)$$

For the contributions from the genuine one-loop triangle diagrams with neutrinos and sneutrinos in the loops to the trilinear Higgs-self coupling in the limit of vanishing momentum we find

$$\begin{aligned}\lambda^{(1,n,\tilde{n})}_{h_i h_j h_k} = &-\frac{1}{16\pi^2}C_0(m^2_{\tilde{n}_{i_1}}, m^2_{\tilde{n}_{i_2}}, m^2_{\tilde{n}_{i_3}})g_{h_i\tilde{n}_{i_1}\tilde{n}_{i_2}}g_{h_j\tilde{n}_{i_1}\tilde{n}_{i_3}}g_{h_k\tilde{n}_{i_2}\tilde{n}_{i_3}} \\ &+\frac{1}{32\pi^2}B^\epsilon_0(m^2_{\tilde{n}_{i_1}}, m^2_{\tilde{n}_{i_2}})\Big(g_{h_i\tilde{n}_{i_1}\tilde{n}_{i_2}}g_{h_j h_k\tilde{n}_{i_1}\tilde{n}_{i_2}} \\ &+g_{h_j\tilde{n}_{i_1}\tilde{n}_{i_2}}g_{h_i h_k\tilde{n}_{i_1}\tilde{n}_{i_2}} + g_{h_k\tilde{n}_{i_1}\tilde{n}_{i_2}}g_{h_i h_j\tilde{n}_{i_1}\tilde{n}_{i_2}}\Big) \\ &+\frac{1}{4\pi^2}\Big[B^\epsilon_0(m^2_{n_{i_1}}, m^2_{n_{i_2}})\Big(\left|g^{L*}_{i_3 i_1 h_i}g^{L*}_{i_3 i_2 h_j}g^L_{i_1 i_2 h_k}\right|m_{n_{i_3}} \\ &+\left|g^{L*}_{i_3 i_1 h_i}g^L_{i_3 i_2 h_k}g^L_{i_1 i_2 h_j}\right|m_{n_{i_1}} \\ &\left|g^{L*}_{i_3 i_1 h_k}g^{L*}_{i_3 i_2 h_j}g^L_{i_1 i_2 h_i}\right|m_{n_{i_3}}\Big) + C_0(m^2_{n_{i_1}}, m^2_{n_{i_2}}, m^2_{n_{i_3}})m_{n_{i_1}} \\ &\Big(\left|g^{L*}_{i_1 i_2 h_i}g^{L*}_{i_3 i_1 h_j}g^L_{i_2 i_3 h_k}\right|m^2_{n_{i_1}}\end{aligned}$$

$$+\left|g^{L*}_{i_1 i_2 h_i} g^{L}_{i_3 i_1 h_j} g^{L*}_{i_2 i_3 h_k}\right| m_{n_{i_1}} m_{n_{i_2}}$$
$$+\left|g^{L}_{i_1 i_2 h_i} g^{L*}_{i_3 i_1 h_j} g^{L*}_{i_2 i_3 h_k}\right| m_{n_{i_1}} m_{n_{i_3}}$$
$$+\left|g^{L*}_{i_1 i_2 h_i} g^{L*}_{i_3 i_1 h_j} g^{L*}_{i_2 i_3 h_k}\right| m_{n_{i_2}} m_{n_{i_3}}\Big)\Big]. \tag{54}$$

The couplings of the neutral Higgs bosons with neutrinos and sneutrinos are derived from the following interaction terms in the Lagrangian

$$i\bar{n}_j(g^{L}_{h_i n_j n_k} P_L + g^{L*}_{h_i n_j n_k} P_R) n_k h_i + i g_{h_i \tilde{n}_j \tilde{n}_k} h_i \tilde{n}_j \tilde{n}_k + i g_{h_i h_j \tilde{n}_k \tilde{n}_l} h_i h_j \tilde{n}_k \tilde{n}_l\,, \tag{55}$$

where

$$\begin{aligned} g^{L}_{h_i n_j n_k} = &-\frac{e^{i\varphi_s}}{\sqrt{2}}\left(\mathcal{R}^{H}_{i,3} + i\mathcal{R}^{H}_{i,6}\right) \\ &\times \sum_{l_2,l_1=1}^{3} (\lambda_X)_{l_1,l_2}\left(\mathcal{U}^{\nu *}_{3,l_2+6}\mathcal{U}^{\nu *}_{k,l_1+6} + \mathcal{U}^{\nu *}_{3,l_1+6}\mathcal{U}^{\nu *}_{k,l_2+6}\right) \\ &-\frac{e^{i\varphi_u}}{\sqrt{2}}\left(\mathcal{R}^{H}_{i,2} + i\mathcal{R}^{H}_{i,5}\right) \\ &\times \sum_{l_2,l_1=1}^{3} Y^{\nu}_{l_1,l_2}\left(\mathcal{U}^{\nu *}_{3,l_2+3}\mathcal{U}^{\nu *}_{k,l_1} + \mathcal{U}^{\nu *}_{3,l_1}\mathcal{U}^{\nu *}_{k,l_2+3}\right). \end{aligned} \tag{56}$$

The couplings between the neutral Higgs bosons and sneutrinos are very lengthy. Therefore we do not display them explicitly here, but we will provide them upon request. The loop functions appearing in the above expressions are given by

$$\begin{aligned} F_0(x,y) &= -x - y\left(3 - 2\ln\overline{x} - \frac{2x\ln\frac{y}{x}}{y-x}\right), \\ A_0(x) &= x(1-\ln\overline{x}), \\ B_0(x,y) &= 1 - \ln\overline{y} - \frac{x\ln\frac{x}{y}}{x-y} \\ B_0(x,x) &= -\ln\overline{x}, \\ B_0(0,x) &= 1 - \ln\overline{x}, \\ B_{00}(x,y) &= \frac{x+y}{4}\left(\frac{3}{2} - \ln\overline{y}\right) - \frac{x}{4}\frac{\ln\frac{x}{y}}{x-y}, \\ B_{00}(x,x) &= \frac{x}{2}(1-\ln\overline{x}), \\ B_{00}(0,x) &= \frac{x}{4}\left(\frac{3}{2} - \ln\overline{x}\right), \quad A^{\epsilon}_0(x) = \frac{x}{\epsilon} + A_0(x), \\ B^{\epsilon}_0(x,y) &= \frac{1}{\epsilon} + B_0(x,y), \\ C_0(x,y,z) &= \frac{y\ln\frac{x}{y}}{(-x+y)(y-z)} + \frac{z\ln\frac{x}{z}}{(-x+z)(-y+z)}, \\ C_0(x,x,x) &= -\frac{1}{2x}, \end{aligned}$$

$$C_0(x,x,z) = \frac{z\ln\left(\frac{x}{z}\right)}{(x-z)^2} - \frac{1}{x-z}, \tag{57}$$

where $\ln\overline{x} = \ln\frac{x}{\mu_R^2}$ with μ_R being the renormalization scale.

4 Numerical analysis

In this section, we analyse the numerical impact of the loop corrections from the (s)neutrino sector to the Higgs trilinear couplings and their correlation with the corrections to the SM-like Higgs boson mass. For this purpose, we have performed a parameter scan where we have taken into account several constraints from the Higgs data, the neutrino oscillation data, the oblique parameters S, T, U, and the charged lepton flavor-violating decays. For our parameter scan we proceed as follows. A given parameter point is first processed by the program `NMSSMCALC-nuSS`. The code calculates the loop-corrected Higgs boson masses in the OS renormalization scheme in the top/stop sector as well as the tree-level SUSY particle masses together with their mixing angles as described in Sect. 2. We require one of the neutral CP-even Higgs bosons to be the SM-like Higgs boson, having a mass in the range

$$122\,\text{GeV} \leq M_{H_{\text{SM}}} \leq 128\,\text{GeV}. \tag{58}$$

Note that we denote H_{SM} as the SM-like Higgs boson, where H_{SM} can be the lightest scalar state H_1 or the next-to-lightest state H_2. The masses of the SUSY particles must be larger than the lower bounds from the LEP and LHC searches [118], in particular we require

$$\begin{aligned} &M_{\chi_1^\pm} > 94\,\text{GeV}, && M_{\chi_2^0} > 62.4\,\text{GeV}, && M_{\chi_3^0} > 99.9\,\text{GeV}, \\ &M_{\chi_4^0} > 116\,\text{GeV}, && M_{\tilde{e}_1} > 107\,\text{GeV}, && M_{\tilde{\mu}_1} > 94\,\text{GeV}, \\ &M_{\tilde{\tau}_1} > 81.9\,\text{GeV}, && M_{\tilde{\nu}_{e/\mu/\tau}} > 94\,\text{GeV}, && M_{\tilde{b}_1} > 1270\,\text{GeV}, \\ &M_{\tilde{t}_1} > 1310\,\text{GeV}, && M_{\tilde{g}} > 2300\,\text{GeV}. \end{aligned} \tag{59}$$

Note, however, that these lower bounds are the most conservative ones from direct searches for the SUSY particles within simplified versions of the MSSM. In most cases, the lightest neutralino is assumed to be the lightest SUSY particle. In some specific cases, there are much stronger bounds existing in literature. `NMSSMCALC-nuSS` provides the Higgs decay widths and branching ratios, including the state-of-the-art higher-order QCD corrections as well as the effective Higgs couplings discussed in Sect. 3. Furthermore, `NMSSMCALC-nuSS` presents all predictions in the SLHA output format which is passed to `HiggsTools` [119], containing `HiggsBounds` [120], to check if the parameter points pass all the exclusion limits from the searches at

Table 1 The input parameter ranges for the scan. The indices i, j run from 1 to 3. All parameters with mass dimension are given in TeV unit

	t_β	λ	κ	M_1, M_2	A_t	$m_{\tilde{Q}_3}, m_{\tilde{t}_R}$	$m_{\tilde{\tau}_R}, m_{\tilde{L}_3}$	$M_{H^\pm}$	A_κ	$\lvert\mu_{\text{eff}}\rvert$
Min	1	0	-1	0.3	-5	1	0.5	0.6	-3	0.2
Max	20	1	1	1	5	3	2	3	3	2
	$(y_\nu)_{ij}$		$(M_X)_{ii}$	$(A_\nu)_{ii}$	$(A_x)_{ii}$	$m_{\tilde{n}_i}, m_{\tilde{x}_i}$	$(B_\mu)_i/(A_x)_{ii}$			
Min	-1		0.5	-2	-2	0	0.001			
Max	1		10	2	2	2	1			

LEP, Tevatron, and the LHC, and `HiggsSignals` [121], to check if the points are consistent with the LHC data for a 125 GeV Higgs boson within 2σ using a χ^2-test. `NMSSMCALC-nuSS` automatically compares its predictions against several experimental results. It can check the neutrino oscillation data, the oblique parameters S, T, U, and the charged lepton flavor-violating decays and decide whether a given parameter point violates any of these constraints. For further information on the use these constraints, we refer the reader to [51] whose strategy is followed here as well.

To efficiently identify phenomenologically viable parameter areas, we make use of the Markov Chain Monte Carlo sampling with `EasyScan_HEP-1.0` [122]. In Table 1, we present the ranges applied for specific parameters appearing in the scan.

Note that we have used the μ_X-parameterization for the neutrino sector. All parameters in Table 1 are chosen to be real in the parameter scan and all the 3×3 matrices are set to be diagonal except for the neutrino Yukawa coupling, y_ν. We assume that the input parameters A_ν, A_X, B_{μ_X} are identical for all three generations. The remaining soft-SUSY-breaking parameters are fixed as follows,

$$M_3 = 2300\,\text{GeV}, \quad m_{\tilde{Q}_{1/2}} = m_{\tilde{L}_{1/2}} = m_{\tilde{x}_R} = 3\,\text{TeV}, \quad A_{b,\tau} = 2\,\text{TeV}, \tag{60}$$

where $x = u, d, c, s, b, e, \mu$. The SM parameters are taken from [118],

$$\begin{aligned} \alpha &= 1/127.955\,, & \alpha_s^{\overline{\text{MS}}}(M_Z) &= 0.1181\,, \\ M_W &= 80.379\,\text{GeV} & M_Z &= 91.1876\,\text{GeV}\,, \\ m_t &= 172.74\,\text{GeV}\,, & m_b^{\overline{\text{MS}}}(m_b^{\overline{\text{MS}}}) &= 4.18\,\text{GeV}\,, \\ m_\tau &= 1.77686\,\text{GeV}\,. \end{aligned} \tag{61}$$

We have selected the normal mass ordering class for the active neutrino inputs. The mass of the lightest neutrino is fixed to be $m_{\nu_1} = 10^{-11}$ GeV while the other neutrino masses and mixing parameters are chosen randomly from the 3σ ranges around their best-fit values,

$$\begin{aligned} m_{\nu_2} &\in \left[\sqrt{m_{\nu_1}^2 + 6.82\times 10^{-23}}, \sqrt{m_{\nu_1}^2 + 8.04\times 10^{-23}}\right]\text{GeV}, \\ m_{\nu_3} &\in \left[\sqrt{m_{\nu_1}^2 + 2.435\times 10^{-21}}, \sqrt{m_{\nu_1}^2 + 2.598\times 10^{-21}}\right]\text{GeV}, \\ \theta_{12} &\in [\arcsin(\sqrt{0.269}), \arcsin(\sqrt{0.343})], \\ \theta_{23} &\in [\arcsin(\sqrt{0.415}), \arcsin(\sqrt{0.617})], \\ \theta_{13} &\in [\arcsin(\sqrt{0.02052}), \arcsin(\sqrt{0.02428})], \\ \delta_{CP} &\in [120, 369]. \end{aligned} \tag{62}$$

In order to study the impact of (s)neutrino contributions on the effective triple Higgs coupling and on the Higgs-to-Higgs decays, we select a valid parameter point from our scan sample and vary each neutrino and sneutrino parameter individually while keeping the other parameters fixed. Note that the variation of the neutrino and sneutrino parameters may lead to a violation of one or more constraints considered in this study. Our chosen parameter point is called `P1`, with the following input parameters:

$$\begin{aligned} M_{H^\pm} &= 1970\,\text{GeV}\,, m_{\tilde{X}} = \text{diag}(806, 1204, 305)\,\text{GeV}\,, \\ M_1 &= 679\,\text{GeV}\,, m_{\tilde{N}} = \text{diag}(337, 157, 359)\,\text{GeV}\,, \\ M_2 &= 461\,\text{GeV}\,, A_\nu = \text{diag}(-678, -678, -678)\,\text{GeV}\,, \\ \mu_{\text{eff}} &= 418\,\text{GeV}\,, A_X = \text{diag}(-1019, -1019, -1019)\,\text{GeV}\,, \\ m_{\tilde{Q}_3} &= 1963\,\text{GeV}\,, B_{\mu_X} = \text{diag}(31, 31, 31)\,\text{GeV}\,, \\ m_{\tilde{t}_R} &= 2203\,\text{GeV}\,, M_X = \text{diag}(5179, 7957, 2527)\,\text{GeV}\,, \\ m_{\tilde{\tau}_R} &= 647\,\text{GeV}\,, ((y_\nu)_{11}, (y_\nu)_{12}, (y_\nu)_{13}) \\ &= (-0.04, -0.48, -0.33)\,, \\ A_t &= -2982\,\text{GeV}\,, ((y_\nu)_{21}, (y_\nu)_{22}, (y_\nu)_{23}) \\ &= (-0.95, 0.35, -0.04)\,, \\ \text{Re}A_k &= -2480\,\text{GeV}\,, ((y_\nu)_{31}, (y_\nu)_{32}, (y_\nu)_{33}) \\ &= (-0.85, 0.07, -0.87)\,, \\ \tan\beta &= 6.4\,, \\ \lambda &= 0.47\,, \kappa = 0.75\,. \end{aligned} \tag{63}$$

The resulting spectrum of the Higgs boson masses at $\mathcal{O}(\alpha_t(\alpha_s + \alpha_t))$ is given in Table 2. For this parameter point, the SM-like Higgs boson is dominated by the h_u component and its mass is about 125.0 GeV, while the second lightest Higgs boson has a mass of 433.3 GeV and is dominantly h_s-like. The remaining Higgs bosons are much heavier.

Table 2 The parameter point P1: Higgs masses in GeV for the NMSSM with and without inverse seesaw mechanism and their main components. The mass spectrum was obtained at two-loop $\mathcal{O}(\alpha_t(\alpha_s+\alpha_t))$ with OS renormalisation in the top/stop sector

	H_1	H_2	H_3	H_4	H_5
ISS	125.0	433.3	1969.4	1971.6	2197.0
No-ISS	123.1	433.3	1969.4	1971.7	2197.0
	h_u	h_s	a	h_d	a_s

4.1 Impact on the SM-like effective triple Higgs coupling and the SM-like Higgs mass

We first investigate the dependence of the effective trilinear coupling $\lambda^{\text{eff}}_{hhh}$ of the SM-like Higgs boson h on a selection of SUSY input parameters. In order to do so, we take the parameter point P1 and vary the chosen input parameter around its central value in P1, cf. Eq. (63). In Fig. 1 (left), we vary the real part of $(A_\nu)_{ii}$ $(i = 1, 2, 3)$ while in Fig. 1 (right) the corresponding complex phases are varied. Note that we have chosen A_ν to be diagonal with the three diagonal entries taken to be identical. The upper panels in Fig. 1 show the effective trilinear Higgs coupling of the SM-like Higgs at one-loop order (red), $\mathcal{O}(\alpha_t\alpha_s)$ (blue) and $\mathcal{O}(\alpha_t(\alpha_s+\alpha_t))$ (black). We remind the reader that the contribution from the (s)neutrino sector only enters at the one-loop level, whereas the two-loop corrections are from the top/stop sector only and do not depend on the neutrino parameters. On the middle panels, we plot the predictions for the SM-like Higgs boson mass at $\mathcal{O}(\alpha_t(\alpha_s+\alpha_t))$ (yellow line) as function of the varied parameters. The predictions for the originally chosen parameter point P1 are presented by the red triangle while all parameter points (obtained from P1 by varying $\text{Re}(A_\nu)_{ii}$) satisfying our applied constraints are denoted by green triangles. Note that the variation of the parameter $(A_\nu)_{ii}$ does not affect the constraints from the neutrino data, but may give a significant effect on the charged lepton flavor-violating decays, the S, T, U parameters and the Higgs signal rates. In the lower panels, we quantify the contribution from the (s)neutrino sector by plotting the relative differences between the results in NMSSMCALC-nuSS and in NMSSMCALC, which is defined as

$$\Delta = \frac{x^{\text{ISS}} - x^{\text{no-ISS}}}{x^{\text{no-ISS}}}, \tag{64}$$

with x^{ISS} ($x^{\text{no-ISS}}$) referring to the SM-like trilinear self-couplings or the Higgs boson mass in the NMSSM with (without) inverse seesaw mechanism at the same loop order. The resulting figure suggests that the trilinear and the Higgs mass values are symmetric around $(A_\nu)_{ii} = 0$, which is, however, not true for the following reasons. The minimal Higgs mass values are obtained for $\text{Re}(A_\nu)_{ii} = \text{Re}(\mu_{\text{eff}})/\tan\beta \sim$ 65 GeV for P1, which corresponds to the off-diagonal components of the sneutrino mass matrix, $M_{\tilde{\nu}_\pm\tilde{N}_\pm}$, being zero. This is similar to the dependence of the one-loop top/stop sector contributions to Higgs boson masses on A_t [104,123]. For the trilinear Higgs self-couplings, however, the dependence on A_ν is more complicated, and the minimal values are obtained for $\text{Re}(A_\nu)_{ii} \sim 30$ GeV. We observe that there are more valid points for negative values of $\text{Re}(A_\nu)_{ii}$ and $\varphi_{(A_\nu)_{ii}}$ than for positive ones. The invalid points violate either the constraints on the charged lepton flavor-violating decays or on the oblique parameters S, T, U. A general feature, as observed in the lower panels of Fig. 1, is that the relative difference in the corrections due to the (s)neutrino sector for the trilinear Higgs self-coupling are two to three times larger (depending on the loop-order) than for the SM-like Higgs mass. In particular, the relative difference in the corrections for the Higgs mass range between 1% and 2.8% for the varied range of $\text{Re}(A_\nu)_{ii}$, while the ones for the trilinear couplings are in [3%,5.8%] at one-loop order, in [3.5%,6.3%] at $\mathcal{O}(\alpha_t\alpha_s)$ and in [2.6%,4.5%] at $\mathcal{O}(\alpha_t(\alpha_s+\alpha_t))$. There exists a strong correlation between the corrections to the SM-like Higgs mass and to the SM-like trilinear Higgs self-coupling. This feature will be discussed at length later in the discussion of Fig. 4. The relative differences in the corrections as defined above give the impression of a rather moderate overall importance of the higher-order corrections to the trilinear coupling. However, this is deceptive because we divide the (s)neutrino corrections by the result obtained in NMSSMCALC at the same considered order thereby accidentally canceling all higher-order contributions from the s/top sector of the denominator with the (s)neutrino contributions in the numerator. If we instead define the (s)neutrino corrections as

$$\delta = (\lambda^{\text{eff,ISS},1L}_{hhh} - \lambda^{\text{eff,no-ISS},1L}_{hhh})/\lambda^{\text{eff,ISS,Tree}}_{hhh}, \tag{65}$$

then we are only sensitive to the higher-order corrections originating from the (s)neutrino sector and find that the one-loop (s)neutrino corrections are in the range of $\delta \propto [7\%, 15\%]$. These large corrections arise from several large neutrino Yukawa coupling components such as $(y_\nu)_{21}, (y_\nu)_{31}, (y_\nu)_{33}$ which are close to one.

We also observe a slight dependence of the trilinear Higgs self-coupling and the SM-like Higgs mass on the phase of $(A_\nu)_{ii}$, as can be inferred from the right panels of Fig. 1. We vary the phase in the range $[-\pi, \pi]$. From the distribution of the green points in the middle right panel it can be seen that the phase $\varphi_{(A_\nu)_{ii}}$ is constrained to very small values. We note that the electric dipole moment (EDM) measurements, which are known to tightly constrain the CP-violating phases in the NMSSM without seesaw mechanism, are not the dominating constraint in this scenario. Most of the points with larger phases pass EDM constraints but violate the S, T, U

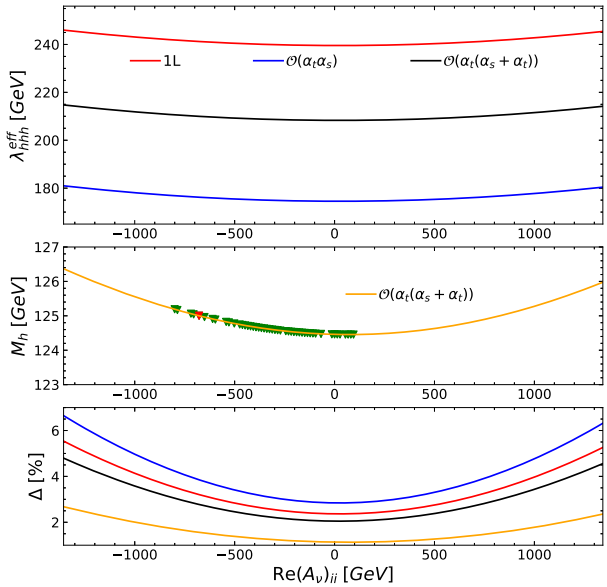

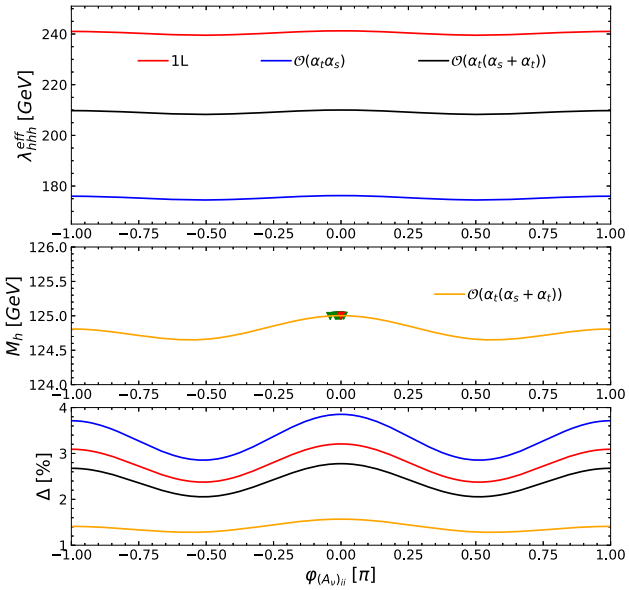

Fig. 1 Upper left panel: the effective trilinear coupling of the SM-like Higgs boson at one-loop order (red), $\mathcal{O}(\alpha_t\alpha_s)$ (blue) and $\mathcal{O}(\alpha_t(\alpha_s+\alpha_t))$ (black) as function of Re$(A_\nu)_{ii}$. Middle left panel: the yellow line presents the SM-like Higgs mass $\mathcal{O}(\alpha_t(\alpha_s+\alpha_t))$ as function of Re$(A_\nu)_{ii}$, the red triangle represents the parameter point P1, green triangles are points satisfying all constraints. Lower left panel: relative changes of the corrections defined in Eq. (64) to the trilinear Higgs self-coupling at the various loop orders (blue, red, black lines) and to the Higgs boson mass at $\mathcal{O}(\alpha_t(\alpha_s+\alpha_t))$ (yellow line) (in percent) due to the (s)neutrino sector. Right plots: similar to left plots but the phase of $(A_\nu)_{ii}$ is varied instead

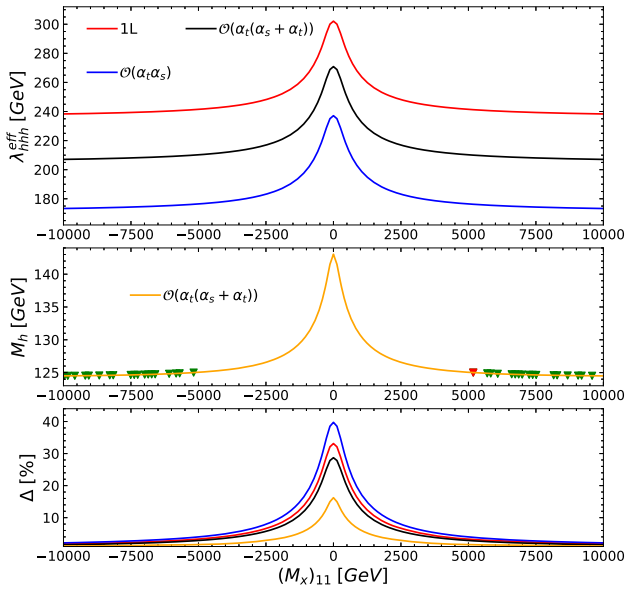

Fig. 2 Similar to Fig. 1 but $(M_X)_{11}$ is varied instead

constraints and/or the constraints from the charged lepton flavor-violating decays.

We next show the impact of M_X on the effective trilinear Higgs self-couplings $\lambda^{\text{eff}}_{hhh}$. In Fig. 2, we present the results with a varying first diagonal component of M_X. The dependence of $\lambda^{\text{eff}}_{hhh}$ and M_h on the other diagonal components is qualitatively the same compared to the one shown here. The notation of Fig. 2 is the same as the one in Fig. 1. The prominent feature of these plots is the peak at $(M_X)_{11} = 0$ in both the mass and the trilinear Higgs coupling plot. While the mass can go up to 143 GeV, the trilinear Higgs coupling at $\mathcal{O}(\alpha_t(\alpha_s+\alpha_t))$ goes up to 271 GeV.[4] The dominant contributions to the corrections on the mass as well on the trilinear Higgs couplings are from the the two lightest sneutrinos and the two lightest heavy neutrinos whose main components are from the singlet superfield $\hat{X}_1$. For this parameter point, the masses of the two lightest sneutrinos are around 378 GeV which are the smallest values for all considered values of $(M_X)_{11}$. They are, however, still not the lightest SUSY particle which is the lightest neutralino with a mass of 368 GeV. The two lightest heavy neutrinos have a mass of 216 GeV. As usual, there is a cancellation between the contributions from fermions and their superpartners. At M_X, the fermions contribute with a positive sign to the scalar diagrams while their superpartners contribute with a negative sign. The neutrino Yukawa coupling component $(y_\nu)_{21} = 0.95$ enlarges these contributions.

From the previous discussion we know that the neutrino Yukawa coupling matrix y_ν is an important factor in the (s)neutrino contributions. In Fig. 3 we present nine plots

[4] We remind the reader that the tree-level SM value is given by $\lambda_{H_{\text{SM}}H_{\text{SM}}H_{\text{SM}}} = 3M^2_{H_{\text{SM}}}/v \approx 190$ GeV.

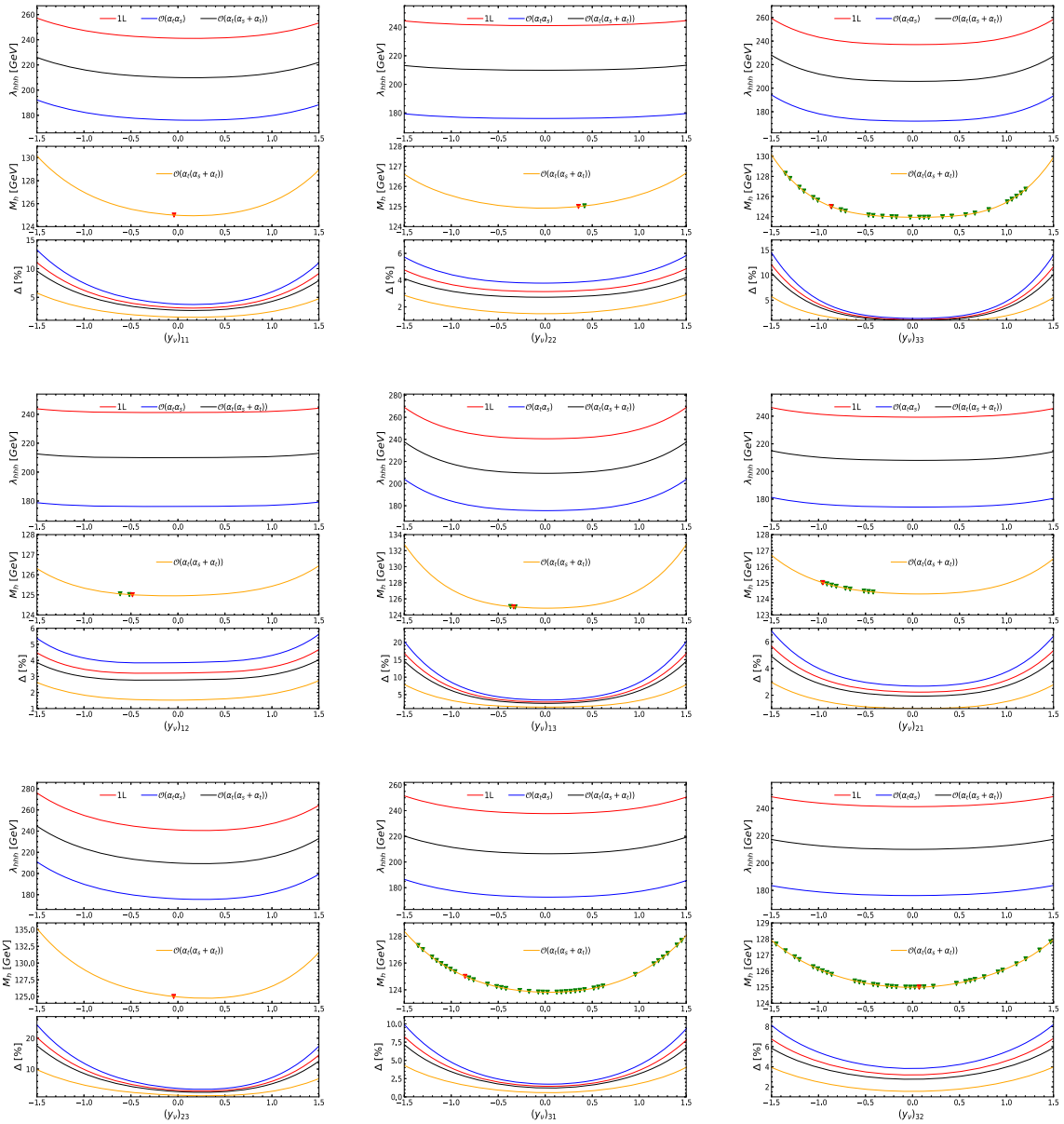

Fig. 3 Dependence of the SM-like triple Higgs self-coupling, the Higgs mass and the relative differences Δ on the nine components of the neutrino Yukawa matrix. The notation and color code is the same as in Fig. 1

in which the nine elements of the matrix y_ν are varied independently. The notation and color code are the same as in the previous plots. We chose the ranges of all varied elements to be $[-1.5, 1.5]$ which is still much smaller than the perturbative unitary limit of $\propto \sqrt{4\pi}$. We observe that the different elements of the matrix affect the trilinear Higgs self-coupling and the mass as well other observables with a different magnitude and shape. For some elements like $(y_\nu)_{11}$, $(y_\nu)_{33}$, $(y_\nu)_{13}$, $(y_\nu)_{23}$, the quantity Δ for $\lambda_{hhh}^{\text{eff}}$ at $\mathcal{O}(\alpha_t(\alpha_s + \alpha_t))$ can be larger than 10%, while for other elements, it remains below 7.5%.

Furthermore, we do not observe a symmetric behaviour around $y_\nu = 0$. We also observe that the constraints from the S, T, U parameters and the charged lepton flavor-violating decays are very sensitive to the change of each element. In particular, we still get a large number of valid points when varying the third row elements $(y_\nu)_{31}$, $(y_\nu)_{32}$, $(y_\nu)_{33}$, which is not the case for the other elements that are in-turn much more strongly constrained. As can be seen from Fig. 3, the variation of each element of the neutrino Yukawa matrix shows a different impact on the THCs as well as on the SM-like Higgs mass. This is due to our initial chosen parameter point P1, which features no symmetric properties in the

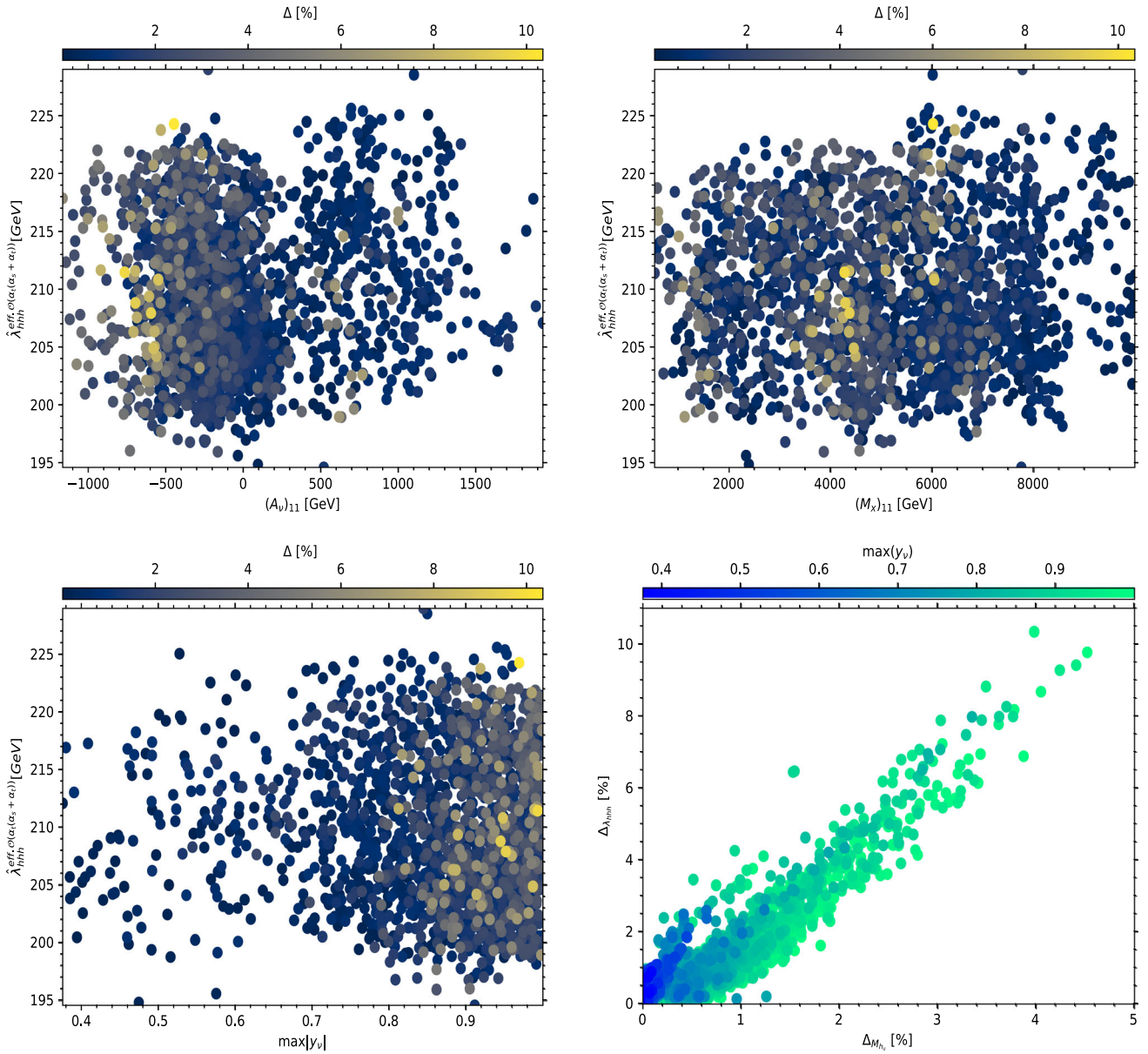

Fig. 4 Scatter plots for the effective SM-like triple Higgs self-couplings (upper and lower left) at $\mathcal{O}(\alpha_t(\alpha_s + \alpha_t))$ for all parameter points obtained from our scan satisfying all our constraints. The color code of each point indicates the relative (s)neutrino correction Δ in percent. The lower right plot shows the correlation between the relative (s)neutrino corrections for the effective SM-like triple Higgs self-coupling and for the SM-like Higgs mass. The color code indicates the maximal absolute value of all neutrino Yukawa coupling elements at each point

matrices y_ν and M_X. If we set y_ν, M_X proportional to the unit matrix, then the three diagonal elements have a similar impact on the THCs and SM-like Higgs mass.

We close this section by showing in Fig. 4 scatter plots obtained in the parameter scan described at the beginning of Sect. 4. In the upper left (upper right / lower left) plot we show the effective trilinear Higgs self-couplings computed at the highest available order as a function of $(A_\nu)_{11}$ ($(M_X)_{11}$ / max$|y_\nu|$), where max$|y_\nu|$ refers to the component of y_ν with the largest absolute value. All parameter points shown in the plots satisfy the applied constraints discussed above. The color of each point represents the magnitude of the relative differences Δ in percent. For all valid points we find that the trilinear Higgs self-coupling $\lambda^{\text{eff}}_{hhh}$ at $\mathcal{O}(\alpha_t(\alpha_s + \alpha_t))$ is in the range of [195, 229] GeV. From these plots, one can infer the preferred regions in the parameters space to get both valid points and maximal (s)neutrino contributions. In the lower right panel, we show a scatter plot with the relative

(s)neutrino corrections computed at $\mathcal{O}(\alpha_t(\alpha_s+\alpha_t))$ for the effective SM-like triple Higgs self-coupling on the vertical axis and the one for the SM-like Higgs mass on the horizontal axis. We observe a strong correlation between these two corrections, similar to the findings in [77], showing that the simultaneous inclusion of higher-order corrections to both quantities can be equally important. For the found parameter points, the values of Δ can go up to 10.5% for the trilinear Higgs self-coupling and up to 4.5% for the Higgs mass, respectively.

An explanation for the strong correlation between the corrections to SM-like THC and the SM-like Higgs mass can be formulated as follows. In the decoupling limit where the masses of all SUSY particles, the charged Higgs, the heavy neutral Higgs masses, the singlet VEV and masses of sterile neutrinos are large compared to the SM mass scale, the SM is a good effective theory of the NMSSM-nuSS. In this limit, one expects that the loop-corrected SM-like Higgs mass and the loop-corrected SM-like triple Higgs coupling are related as in the SM, i.e. $\lambda_{\rm SM} = 3M_H^2/v$. The corrections defined in Eq. (64) to the triple Higgs coupling and to the Higgs mass can be approximated as

$$\Delta_\lambda = \frac{\lambda_{hhh}^{\rm eff,ISS} - \lambda_{hhh}^{\rm eff,no\text{-}ISS}}{\lambda_{hhh}^{\rm eff,no\text{-}ISS}} \sim \frac{(M_h^{\rm ISS})^2 - (M_h^{\rm no\text{-}ISS})^2}{(M_h^{\rm no\text{-}ISS})^2} \sim 2\Delta_{M_h}. \tag{66}$$

Many valid points obtained from our scan on the lower right plot of Fig. 4 are aligned along the line $\Delta_\lambda \sim 2\Delta_{M_h}$. However, there are also points which do not follow the above estimate. We quantify the genuine correction to the triple Higgs coupling by the difference $\Delta_\lambda - 2\Delta_{M_h}$, which is in the range $[-2.3, 3.4]$% for all valid points. Investigating the outliers, we find that these points have rather low masses for the sterile neutrinos and their corresponding superpartners, as well as a significant mixing among the sneutrinos. For these points the cancellation between the contributions from the neutrinos and the contributions from the sneutrinos can be strong either in the mass corrections or in the trilinear coupling corrections, but not simultaneously in both predictions.

4.2 Impacts on Higgs-to-Higgs decays

In this section we present our new results for the Higgs-to-Higgs decay widths and branching ratios implemented in the code `NMSSMCALC-nuSS`. We first investigate the parameter point `P1`, cf. Table 2. In Table 3 we show all kinematically allowed Higgs decay channels with the predictions for their corresponding branching ratios at tree-level, one-loop order, $\mathcal{O}(\alpha_t\alpha_s)$ and $\mathcal{O}(\alpha_t(\alpha_s+\alpha_t))$ in the NMSSM with inverse seesaw mechanism. For comparison, we present in the last row results for the branching ratios at $\mathcal{O}(\alpha_t(\alpha_s+\alpha_t))$ obtained in the NMSSM without inverse seesaw mechanism. Note that the Higgs-to-Higgs decay widths are defined in Eq. (34) and that we dress *all* results with the external-leg corrections in order to ensure the fields are on the mass shell. This means in particular, that, in the defined tree-level accuracy, we include partially higher-order effects through the WFR factor $\mathbf{Z}^H$. As we can see, there is a significant change of the branching ratios when we compare the tree-level to the one-loop results. Especially for the decay channel $H_2 \to H_1H_1$, the one-loop result is about 40% larger than the tree-level one. However, for the remaining decay channels, the branching ratios are reduced when the higher-order corrections to the decay widths are included. The effect of the (s)neutrino contributions on the branching ratios can be roughly estimated by comparing the branching ratios between the models with and without ISS at the same order of accuracy. The contributions entering the decay widths can be classified into three parts: the Higgs masses, the WFR factor and the one-loop diagrams. Since the effect from the (s)neutrino sector is mostly related to the neutrino Yukawa couplings, which are the couplings between the doublet Higgs H_u and the left-handed neutrinos and N-neutrinos, one expects that their effect may be small for the decays of the non-SM-like Higgs bosons. From the two last rows in Table 3, one can see that the new contributions are indeed small on the branching ratios. The relative differences Δ are largest for the decay $H_4 \to H_1H_1$ with about 3.4%.

We also investigate the dependence of the Higgs-to-Higgs decay widths on parameters of the (s)neutrino sector and demonstrate the significant effect coming from the neutrino Yukawa couplings. All other parameters are found to give small or mild effects. To illustrate our findings we present in Fig. 5 the dependence of the five decay widths $\Gamma(H_2 \to H_1H_1)$, $\Gamma(H_4 \to H_1H_1)$, $\Gamma(H_4 \to H_1H_2)$, $\Gamma(H_4 \to H_2H_2)$, and $\Gamma(H_5 \to H_1H_3)$ on the first component of the neutrino Yukawa matrix, $(y_\nu)_{11}$, which is varied in the range $[-1.5, 1.5]$. The green, red, blue, and black lines in the upper panels of each plot represent the decay widths at tree-level, one-loop order, $\mathcal{O}(\alpha_t\alpha_s)$, and $\mathcal{O}(\alpha_t(\alpha_s+\alpha_t))$, respectively. We see that the tree-level decay widths also depend on $(y_\nu)_{11}$. This dependence stems from the WFR factors and the phase-space factor and is quite noticeable for most of the considered decay channels. In the lower panels of each plot, we show the absolute value of the relative (s)neutrino corrections defined as

$$\delta^x = \left| \frac{\Gamma^{x,\rm ISS} - \Gamma^{x,\rm noISS}}{\Gamma^{x-1,\rm ISS}} \right| \tag{67}$$

with x denoting the level of accuracy (1 L/$\mathcal{O}(\alpha_t\alpha_s)$/$\mathcal{O}(\alpha_t(\alpha_s+\alpha_t))$ corresponding to the (red/blue/black colors) and $x-1$ being the next-lower level of accuracy. With this definition, the nominator of Eq. (67) represents the (s)neutrino contributions to the width at the considered order. For all decays

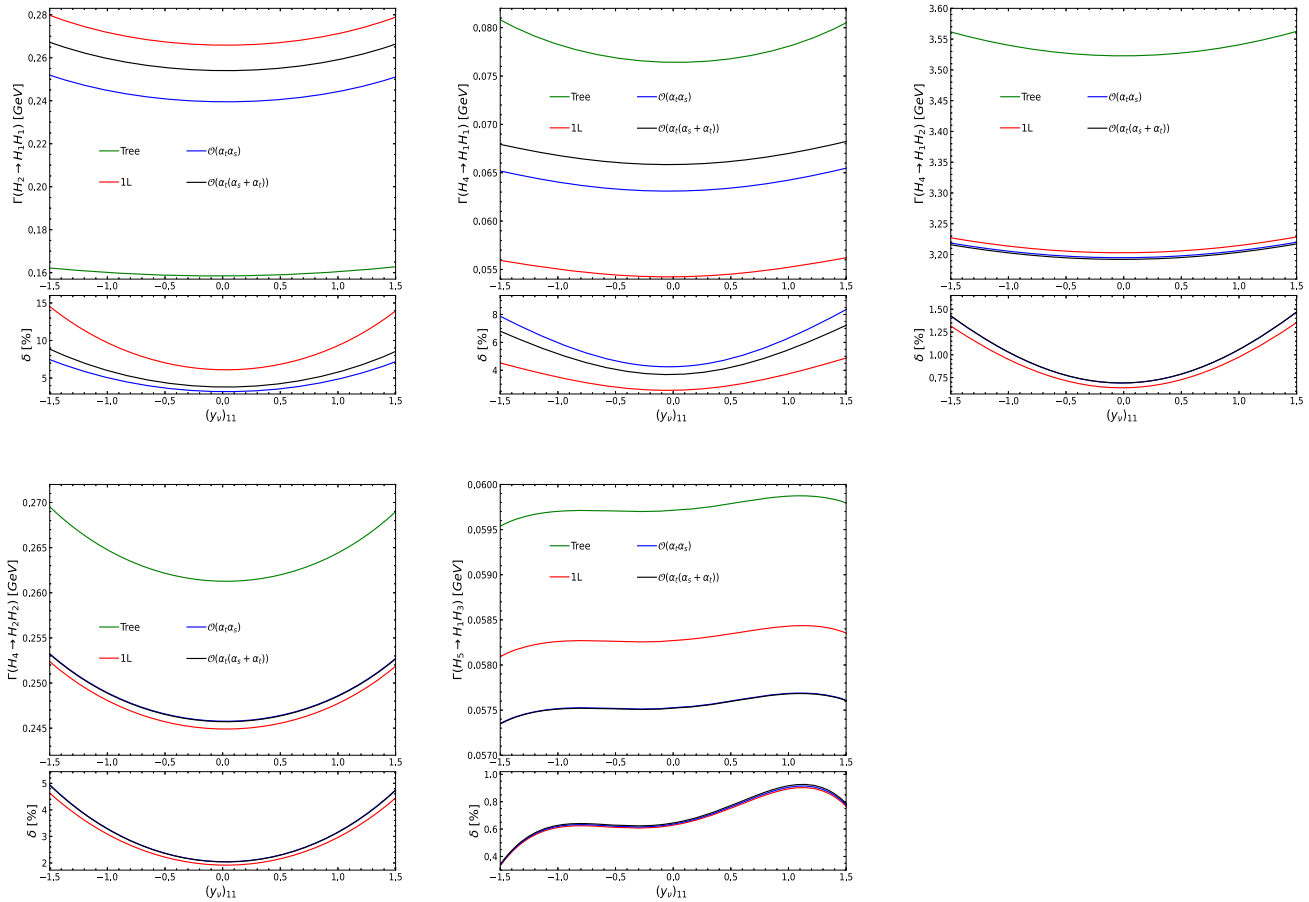

Fig. 5 Upper panels: The decay widths at tree-level (green), one-loop (red), two-loop QCD $\mathcal{O}(\alpha_t\alpha_s)$ (blue) and two-loop EW $\mathcal{O}(\alpha_t(\alpha_t+\alpha_s))$ (black) for $H_2 \to H_1H_1$, $H_4 \to H_1H_1$, $H_4 \to H_1H_2$, $H_4 \to H_2H_2$, $H_5 \to H_1H_3$ as functions of the first component of the neutrino Yukawa matrix, $(y_\nu)_{11}$. Lower panels: Absolute values of the relative (s)neutrino corrections as defined in Eq. (67)

Table 3 The parameter point `P1`: all possible Higgs-to-Higgs decays and their branching ratios in percent at several levels of accuracy in the NMSSM with and without inverse seesaw mechanism

	$\text{Br}(H_2 \to H_1H_1)$	$\text{Br}(H_4 \to H_1H_1)$	$\text{Br}(H_4 \to H_1H_2)$	$\text{Br}(H_4 \to H_2H_2)$	$\text{Br}(H_5 \to H_1H_3)$
Tree-level-ISS	26.35	0.247	11.39	0.845	0.335
One-loop-ISS	37.52	0.177	10.47	0.801	0.327
$\mathcal{O}(\alpha_t\alpha_s)$-ISS	35.11	0.206	10.45	0.804	0.323
$\mathcal{O}(\alpha_t(\alpha_s+\alpha_t))$-ISS	36.46	0.215	10.44	0.804	0.323
$\mathcal{O}(\alpha_t(\alpha_s+\alpha_t))$-no-ISS	36.03	0.208	10.38	0.788	0.321

considered here, δ^{1L} is the largest for the $H_2 \to H_1H_1$ decay channel, which involves two SM-like Higgs bosons in the final states. The correction to this particular channel is in the range $[7, 14.5]\%$ for the varied range of $(y_\nu)_{11}$, while it remains below 5% for the other decays. The qualitative behaviour of δ at $\mathcal{O}(\alpha_t\alpha_s)$ and $\mathcal{O}(\alpha_t(\alpha_s+\alpha_t))$ is quite similar to the one-loop one with different magnitudes. This is because the nominators of Eq. (67) are quite close to the one-loop results, as the leading higher-order effects are independent of the ISS mechanism and therefore drop out, while the higher-orders entering the denominator are different and not cancelled. For all plots in Fig. 5, the dependence of the widths and δ on $(y_\nu)_{11}$ for the decay $H_5 \to H_1H_3$ looks different than the ones for the other decays. In particular, the width of $H_5 \to H_1H_3$ is smallest at $(y_\nu)_{11} = -1.5$ while it is the largest here for the other decays. This is due to the phase space factor R_2 which is smallest at $(y_\nu)_{11} = -1.5$.

5 Conclusions

In this paper we investigated the influence of the inverse seesaw mechanism in the NMSSM for both the higher-order corrections to the effective trilinear Higgs self-couplings and the Higgs-to-Higgs decays in comparison with the corrections on the Higgs boson masses. We computed the complete one-loop corrections to the Higgs-to-Higgs decay widths taking into account non-vanishing external momentum. Furthermore, we obtain the dominant one-loop corrections from the (s)top sector and the (s)neutrino sector to the effective SM-like trilinear Higgs self-coupling computed in the limit of vanishing external momenta and in the limit of vanishing gauge couplings. Regarding the renormalization, we applied a mixed OS-$\overline{\text{DR}}$ scheme, which is the same scheme used for the loop-corrections to the Higgs boson masses. We then consistently combined the one-loop result with the leading two-loop $\mathcal{O}(\alpha_t\alpha_s)$ and $\mathcal{O}(\alpha_t(\alpha_s+\alpha_t))$ results previously computed in the vanilla NMSSM by our group. In the numerical analysis, we performed a parameter scan of the model and kept only those points for our study that respect the constraints from the Higgs data, the neutrino oscillation data, the charged lepton flavor-violating decays $l_i \to l_j + \gamma$, and the new physics constraints from the oblique parameters S, T, U. We quantify the impact of the one-loop corrections from the (s)neutrino sector on the SM-like Higgs trilinear self-coupling and on the SM-like Higgs boson mass prediction by defining the relative differences Δ between the results with and without (s)neutrino contributions. We find that the Δ for the SM-like trilinear Higgs self-coupling can reach 10.5% while the relative corrections to the SM-like Higgs boson mass can reach reach 4.5% for all found parameter points. The relative effect of (s)neutrinos on the decay widths of the heavy Higgs decays can be significant for the decays of the singlet-like and down-type-like scalars decaying into a pair of the SM-like Higgs bosons. For the Higgs-to-Higgs branching ratios of non-SM-like Higgs bosons, Δ is less than 3.4% and mostly encoded in the external-leg corrections and phase-space factors.

Acknowledgements M.M. acknowledges support by the Deutsche Forschungsgemeinschaft (DFG, German Research Foundation) under grant 396021762 - TRR 257.

Data Availability Statement This manuscript has no associated data. [Authors' comment: The input parameters are given in the paper and all the numerical results are either given in the tables or displayed in the figures.]

Code Availability Statement This manuscript has no associated code/software. [Authors' comment: The code/software generated during and/or analysed during the current study is publicly available at https://www.itp.kit.edu/~maggie/NMSSMCALC-nuSS/.]

Funded by SCOAP[3].

References

1. ATLAS Collaboration, G. Aad et al., Observation of a new particle in the search for the Standard Model Higgs boson with the ATLAS detector at the LHC. Phys. Lett. B **716**, 1–29 (2012). https://doi.org/10.1016/j.physletb.2012.08.020. arXiv:1207.7214
2. CMS Collaboration, S. Chatrchyan et al., Observation of a new boson at a mass of 125 GeV with the CMS Experiment at the LHC. Phys. Lett. B **716**, 30–61 (2012). https://doi.org/10.1016/j.physletb.2012.08.021. arXiv:1207.7235
3. ATLAS Collaboration, G. Aad et al., A detailed map of Higgs boson interactions by the ATLAS experiment ten years after the discovery. Nature **607**, 52–59 (2022). https://doi.org/10.1038/s41586-022-04893-w. arXiv:2207.00092
4. CMS Collaboration, A. Tumasyan et al., A portrait of the Higgs boson by the CMS experiment ten years after the discovery. Nature **607**, 60–68 (2022). https://doi.org/10.1038/s41586-022-04892-x. arXiv:2207.00043
5. Super-Kamiokande Collaboration, Y. Fukuda et al., Evidence for oscillation of atmospheric neutrinos. Phys. Rev. Lett. **81**, 1562–1567 (1998). https://doi.org/10.1103/PhysRevLett.81.1562. arXiv:hep-ex/9807003
6. R.N. Mohapatra, Mechanism for understanding small neutrino mass in superstring theories. Phys. Rev. Lett. **56**, 561–563 (1986). https://doi.org/10.1103/PhysRevLett.56.561
7. R.N. Mohapatra, J.W.F. Valle, Neutrino mass and baryon number nonconservation in superstring models. Phys. Rev. D **34**, 1642 (1986). https://doi.org/10.1103/PhysRevD.34.1642
8. Y. Golfand, E. Likhtman, Extension of the algebra of Poincare group generators and violation of p invariance. JETP Lett. **13**, 323–326 (1971)
9. D.V. Volkov, V.P. Akulov, Is the neutrino a goldstone particle? Phys. Lett. B **46**, 109–110 (1973). https://doi.org/10.1016/0370-2693(73)90490-5
10. J. Wess, B. Zumino, Supergauge transformations in four-dimensions. Nucl. Phys. B **70**, 39–50 (1974). https://doi.org/10.1016/0550-3213(74)90355-1
11. P. Fayet, Supergauge invariant extension of the Higgs mechanism and a model for the electron and its neutrino. Nucl. Phys. B **90**, 104–124 (1975). https://doi.org/10.1016/0550-3213(75)90636-7
12. P. Fayet, Spontaneously broken supersymmetric theories of weak, electromagnetic and strong interactions. Phys. Lett. B **69**, 489 (1977). https://doi.org/10.1016/0370-2693(77)90852-8
13. P. Fayet, S. Ferrara, Supersymmetry. Phys. Rep. **32**, 249–334 (1977). https://doi.org/10.1016/0370-1573(77)90066-7
14. H.P. Nilles, M. Srednicki, D. Wyler, Weak interaction breakdown induced by supergravity. Phys. Lett. B **120**, 346 (1983). https://doi.org/10.1016/0370-2693(83)90460-4
15. H.P. Nilles, Supersymmetry, supergravity and particle physics. Phys. Rep. **110**, 1–162 (1984). https://doi.org/10.1016/0370-1573(84)90008-5

16. J. Frere, D. Jones, S. Raby, Fermion masses and induction of the weak scale by supergravity. Nucl. Phys. B **222**, 11 (1983). https://doi.org/10.1016/0550-3213(83)90606-5
17. J. Derendinger, C.A. Savoy, Quantum effects and SU(2) x U(1) breaking in supergravity Gauge theories. Nucl. Phys. B **237**, 307 (1984). https://doi.org/10.1016/0550-3213(84)90162-7
18. H.E. Haber, G.L. Kane, The search for supersymmetry: probing physics beyond the standard model. Phys. Rep. **117**, 75–263 (1985). https://doi.org/10.1016/0370-1573(85)90051-1
19. M. Sohnius, Introducing supersymmetry. Phys. Rep. **128**, 39–204 (1985). https://doi.org/10.1016/0370-1573(85)90023-7
20. J.F. Gunion, H.E. Haber, Higgs Bosons in supersymmetric models. 1. Nucl. Phys. B **272**, 1 (1986). https://doi.org/10.1016/0550-3213(86)90340-8
21. J.F. Gunion, H.E. Haber, Higgs Bosons in supersymmetric models. 2. Implications for phenomenology. Nucl. Phys. B **278**, 449 (1986). https://doi.org/10.1016/0550-3213(86)90050-7
22. P. Slavich et al., Higgs-mass predictions in the MSSM and beyond. Eur. Phys. J. C **81**, 450 (2021). https://doi.org/10.1140/epjc/s10052-021-09198-2. arXiv:2012.15629
23. E.A.R. Reyes, R. Fazio, High-precision calculations of the Higgs Boson mass. Particles **5**, 53–73 (2022). https://doi.org/10.3390/particles5010006. arXiv:2112.15295
24. J.F. Gunion, H.E. Haber, G.L. Kane, S. Dawson, The Higgs Hunter's Guide, vol. 80 (2000). https://doi.org/10.1201/9780429496448
25. S.P. Martin, A supersymmetry primer. Adv. Ser. Direct. High Energy Phys. **18**, 1–98 (1998). https://doi.org/10.1142/9789812839657_0001. arXiv:hep-ph/9709356
26. S. Dawson, The MSSM and why it works. in *Theoretical Advanced Study Institute in Elementary Particle Physics (TASI 97): Supersymmetry, Supergravity and Supercolliders*, vol. 6 (1997), pp. 261–339. arXiv:hep-ph/9712464
27. A. Djouadi, The anatomy of electro-weak symmetry breaking. II. The Higgs bosons in the minimal supersymmetric model. Phys. Rep. **459**, 1–241 (2008). https://doi.org/10.1016/j.physrep.2007.10.005. arXiv:hep-ph/0503173
28. S. Heinemeyer, M.J. Herrero, S. Penaranda, A.M. Rodriguez-Sanchez, Higgs boson masses in the MSSM with heavy Majorana neutrinos. JHEP **05**, 063 (2011). https://doi.org/10.1007/JHEP05(2011)063. arXiv:1007.5512
29. P. Draper, H.E. Haber, Decoupling of the right-handed neutrino contribution to the Higgs mass in supersymmetric models. Eur. Phys. J. C **73**, 2522 (2013). https://doi.org/10.1140/epjc/s10052-013-2522-7. arXiv:1304.6103
30. E.J. Chun, V.S. Mummidi, S.K. Vempati, Anatomy of Higgs mass in supersymmetric inverse seesaw models. Phys. Lett. B **736**, 470–477 (2014). https://doi.org/10.1016/j.physletb.2014.08.002. arXiv:1405.5478
31. I. Gogoladze, B. He, A. Mustafayev, S. Raza, Q. Shafi, Effects of neutrino inverse seesaw mechanism on the Sparticle spectrum in CMSSM and NUHM2. JHEP **05**, 078 (2014). https://doi.org/10.1007/JHEP05(2014)078. arXiv:1401.8251
32. T. Biekötter, S. Heinemeyer, C. Muñoz, Precise prediction for the Higgs-boson masses in the $\mu\nu$ SSM. Eur. Phys. J. C **78**, 504 (2018). https://doi.org/10.1140/epjc/s10052-018-5978-7. arXiv:1712.07475
33. T. Biekötter, S. Heinemeyer, C. Muñoz, Precise prediction for the Higgs-boson masses in the $\mu\nu$ SSM with three right-handed neutrino superfields. Eur. Phys. J. C **79**, 667 (2019). https://doi.org/10.1140/epjc/s10052-019-7175-8. arXiv:1906.06173
34. M. Dine, W. Fischler, M. Srednicki, A simple solution to the strong CP problem with a harmless axion. Phys. Lett. B **104**, 199 (1981). https://doi.org/10.1016/0370-2693(81)90590-6
35. R. Barbieri, S. Ferrara, C.A. Savoy, Gauge models with spontaneously broken local supersymmetry. Phys. Lett. B **119**, 343 (1982). https://doi.org/10.1016/0370-2693(82)90685-2
36. J.R. Ellis, J. Gunion, H.E. Haber, L. Roszkowski, F. Zwirner, Higgs bosons in a nonminimal supersymmetric model. Phys. Rev. D **39**, 844 (1989). https://doi.org/10.1103/PhysRevD.39.844
37. M. Drees, Supersymmetric models with extended Higgs sector. Int. J. Mod. Phys. A **4**, 3635 (1989). https://doi.org/10.1142/S0217751X89001448
38. U. Ellwanger, M. Rausch de Traubenberg, C.A. Savoy, Particle spectrum in supersymmetric models with a gauge singlet. Phys. Lett. B **315**, 331–337 (1993). https://doi.org/10.1016/0370-2693(93)91621-S. arXiv:hep-ph/9307322
39. U. Ellwanger, M. Rausch de Traubenberg, C.A. Savoy, Higgs phenomenology of the supersymmetric model with a gauge singlet. Z. Phys. C **67**, 665–670 (1995). https://doi.org/10.1007/BF01553993. arXiv:hep-ph/9502206
40. U. Ellwanger, M. Rausch de Traubenberg, C.A. Savoy, Phenomenology of supersymmetric models with a singlet. Nucl. Phys. B **492**, 21–50 (1997). https://doi.org/10.1016/S0550-3213(97)00128-4. arXiv:hep-ph/9611251
41. T. Elliott, S. King, P. White, Unification constraints in the next-to-minimal supersymmetric standard model. Phys. Lett. B **351**, 213–219 (1995). https://doi.org/10.1016/0370-2693(95)00381-T. arXiv:hep-ph/9406303
42. S. King, P. White, Resolving the constrained minimal and next-to-minimal supersymmetric standard models. Phys. Rev. D **52**, 4183–4216 (1995). https://doi.org/10.1103/PhysRevD.52.4183. arXiv:hep-ph/9505326
43. F. Franke, H. Fraas, Neutralinos and Higgs bosons in the next-to-minimal supersymmetric standard model. Int. J. Mod. Phys. A **12**, 479–534 (1997). https://doi.org/10.1142/S0217751X97000529. arXiv:hep-ph/9512366
44. M. Maniatis, The next-to-minimal supersymmetric extension of the standard model reviewed. Int. J. Mod. Phys. A **25**, 3505–3602 (2010). https://doi.org/10.1142/S0217751X10049827. arXiv:0906.0777
45. U. Ellwanger, C. Hugonie, A.M. Teixeira, The next-to-minimal supersymmetric standard model. Phys. Rep. **496**, 1–77 (2010). https://doi.org/10.1016/j.physrep.2010.07.001. arXiv:0910.1785
46. U. Ellwanger, Phenomenological aspects of the next-to-minimal supersymmetric standard model. arXiv:0908.4231 [v1]
47. C. Balazs, M. Carena, A. Freitas, C.E.M. Wagner, Phenomenology of the nMSSM from colliders to cosmology. JHEP **06**, 066 (2007). https://doi.org/10.1088/1126-6708/2007/06/066. arXiv:0705.0431
48. I. Gogoladze, N. Okada, Q. Shafi, NMSSM and seesaw physics at LHC. Phys. Lett. B **672**, 235–239 (2009). https://doi.org/10.1016/j.physletb.2008.12.068. arXiv:0809.0703
49. I. Gogoladze, B. He, Q. Shafi, Inverse seesaw in NMSSM and 126 GeV Higgs boson. Phys. Lett. B **718**, 1008–1013 (2013). https://doi.org/10.1016/j.physletb.2012.11.043. arXiv:1209.5984
50. W. Wang, J.M. Yang, L.L. You, Higgs boson mass in NMSSM with right-handed neutrino. JHEP **07**, 158 (2013). https://doi.org/10.1007/JHEP07(2013)158. arXiv:1303.6465
51. T.N. Dao, M. Mühlleitner, A.V. Phan, Loop-corrected Higgs masses in the NMSSM with inverse seesaw mechanism. Eur. Phys. J. C **82**, 667 (2022). https://doi.org/10.1140/epjc/s10052-022-10590-9. arXiv:2108.10088
52. T.N. Dao, D.N. Le, M. Mühlleitner, Leptonic anomalous magnetic and electric dipole moments in the CP-violating NMSSM with and without inverse seesaw mechanism. Eur. Phys. J. C **82**, 954 (2022). https://doi.org/10.1140/epjc/s10052-022-10928-3. arXiv:2207.12618
53. A. Djouadi, W. Kilian, M. Muhlleitner, P.M. Zerwas, Testing Higgs selfcouplings at e+ e- linear colliders. Eur. Phys.

J. C **10**, 27–43 (1999). https://doi.org/10.1007/s100529900082. arXiv:hep-ph/9903229
54. A. Djouadi, W. Kilian, M. Muhlleitner, P.M. Zerwas, Production of neutral Higgs boson pairs at LHC. Eur. Phys. J. C **10**, 45–49 (1999). https://doi.org/10.1007/s100529900083. arXiv:hep-ph/9904287
55. M.M. Muhlleitner, Higgs particles in the standard model and supersymmetric theories. PhD thesis, Hamburg U. (2000). arXiv:hep-ph/0008127
56. J. Alison et al., Higgs boson potential at colliders: status and perspectives. Rev. Phys. **5**, 100045 (2020). https://doi.org/10.1016/j.revip.2020.100045. arXiv:1910.00012
57. ATLAS Collaboration, G. Aad et al., Combination of searches for Higgs boson pair production in pp collisions at $\sqrt{s} = 13$ TeV with the ATLAS detector. arXiv:2406.09971
58. H. Abouabid, A. Arhrib, D. Azevedo, J.E. Falaki, P.M. Ferreira, M. Mühlleitner et al., Benchmarking di-Higgs production in various extended Higgs sector models. JHEP **09**, 011 (2022). https://doi.org/10.1007/JHEP09(2022)011. arXiv:2112.12515
59. ATLAS Collaboration, HL-LHC prospects for the measurement of Higgs boson pair production in the $b\bar{b}b\bar{b}$ final state and combination with the $b\bar{b}\gamma\gamma$ and $b\bar{b}\tau^+\tau^-$ final states at the ATLAS experiment. CERN, Geneva (2022)
60. C.F. Dürig, Measuring the Higgs self-coupling at the international linear collider. PhD thesis, Hamburg U., Hamburg (2016). https://doi.org/10.3204/PUBDB-2016-04283
61. H. Abramowicz et al., Higgs physics at the CLIC electron–positron linear collider. Eur. Phys. J. C **77**, 475 (2017). https://doi.org/10.1140/epjc/s10052-017-4968-5. arXiv:1608.07538
62. CLICdp Collaboration, P. Roloff, U. Schnoor, R. Simoniello, B. Xu, Double Higgs boson production and Higgs self-coupling extraction at CLIC. Eur. Phys. J. C **80**, 1010 (2020). https://doi.org/10.1140/epjc/s10052-020-08567-7. arXiv:1901.05897
63. M.L. Mangano, G. Ortona, M. Selvaggi, Measuring the Higgs self-coupling via Higgs-pair production at a 100 TeV p-p collider. Eur. Phys. J. C **80**, 1030 (2020). https://doi.org/10.1140/epjc/s10052-020-08595-3. arXiv:2004.03505
64. F. Arco, S. Heinemeyer, M. Mühlleitner, K. Radchenko, Sensitivity to triple Higgs couplings via di-Higgs production in the 2HDM at the (HL-)LHC. Eur. Phys. J. C **83**, 1019 (2023). https://doi.org/10.1140/epjc/s10052-023-12193-4. arXiv:2212.11242
65. S. Heinemeyer, M. Mühlleitner, K. Radchenko, G. Weiglein, Higgs pair production in the 2HDM: impact of loop corrections to the trilinear Higgs couplings and interference effects on experimental limits. arXiv:2403.14776
66. F. Feuerstake, E. Fuchs, T. Robens, D. Winterbottom, Interference effects in resonant di-Higgs production at the LHC in the Higgs singlet extension. arXiv:2409.06651
67. W. Hollik, S. Penaranda, Yukawa coupling quantum corrections to the selfcouplings of the lightest MSSM Higgs boson. Eur. Phys. J. C **23**, 163–172 (2002). https://doi.org/10.1007/s100520100862. arXiv:hep-ph/0108245
68. E. Senaha, Radiative corrections to triple Higgs coupling and electroweak phase transition: beyond one-loop analysis. Phys. Rev. D **100**, 055034 (2019). https://doi.org/10.1103/PhysRevD.100.055034. arXiv:1811.00336
69. J. Braathen, S. Kanemura, On two-loop corrections to the Higgs trilinear coupling in models with extended scalar sectors. Phys. Lett. B **796**, 38–46 (2019). https://doi.org/10.1016/j.physletb.2019.07.021. arXiv:1903.05417
70. V.D. Barger, M.S. Berger, A.L. Stange, R.J.N. Phillips, Supersymmetric Higgs boson hadroproduction and decays including radiative corrections. Phys. Rev. D **45**, 4128–4147 (1992). https://doi.org/10.1103/PhysRevD.45.4128
71. A. Dobado, M.J. Herrero, W. Hollik, S. Penaranda, Selfinteractions of the lightest MSSM Higgs boson in the large pseudoscalar mass limit. Phys. Rev. D **66**, 095016 (2002). https://doi.org/10.1103/PhysRevD.66.095016. arXiv:hep-ph/0208014
72. K.E. Williams, G. Weiglein, Precise predictions for $h_a \to h_b h_c$ decays in the complex MSSM. Phys. Lett. B **660**, 217–227 (2008). https://doi.org/10.1016/j.physletb.2007.12.049. arXiv:0710.5320
73. K.E. Williams, H. Rzehak, G. Weiglein, Higher order corrections to Higgs boson decays in the MSSM with complex parameters. Eur. Phys. J. C **71**, 1669 (2011). https://doi.org/10.1140/epjc/s10052-011-1669-3. arXiv:1103.1335
74. M. Brucherseifer, R. Gavin, M. Spira, Minimal supersymmetric Higgs boson self-couplings: two-loop $O(\alpha_t\alpha_s)$ corrections. Phys. Rev. D **90**, 117701 (2014). https://doi.org/10.1103/PhysRevD.90.117701. arXiv:1309.3140
75. D.T. Nhung, M. Muhlleitner, J. Streicher, K. Walz, Higher order corrections to the trilinear Higgs self-couplings in the real NMSS. JHEP **11**, 181 (2013). https://doi.org/10.1007/JHEP11(2013)181. arXiv:1306.3926
76. M. Mühlleitner, D.T. Nhung, H. Ziesche, The order $\mathcal{O}(\alpha_t\alpha_s)$ corrections to the trilinear Higgs self-couplings in the complex NMSSM. JHEP **12**, 034 (2015). https://doi.org/10.1007/JHEP12(2015)034. arXiv:1506.03321
77. C. Borschensky, T.N. Dao, M. Gabelmann, M. Mühlleitner, H. Rzehak, The trilinear Higgs self-couplings at $\mathcal{O}(\alpha_t^2)$ in the CP-violating NMSSM. Eur. Phys. J. C **83**, 118 (2023). https://doi.org/10.1140/epjc/s10052-023-11215-5. arXiv:2210.02104
78. J. Baglio, T.N. Dao, M. Mühlleitner, One-loop corrections to the two-body decays of the neutral Higgs bosons in the complex NMSSM. arXiv:1907.12060
79. S. Kanemura, S. Kiyoura, Y. Okada, E. Senaha, C.P. Yuan, New physics effect on the Higgs selfcoupling. Phys. Lett. B **558**, 157–164 (2003). https://doi.org/10.1016/S0370-2693(03)00268-5. arXiv:hep-ph/0211308
80. S. Kanemura, Y. Okada, E. Senaha, C.P. Yuan, Higgs coupling constants as a probe of new physics. Phys. Rev. D **70**, 115002 (2004). https://doi.org/10.1103/PhysRevD.70.115002. arXiv:hep-ph/0408364
81. S. Kanemura, M. Kikuchi, K. Yagyu, Fingerprinting the extended Higgs sector using one-loop corrected Higgs boson couplings and future precision measurements. Nucl. Phys. B **896**, 80–137 (2015). https://doi.org/10.1016/j.nuclphysb.2015.04.015. arXiv:1502.07716
82. S. Kanemura, M. Kikuchi, K. Sakurai, K. Yagyu, Gauge invariant one-loop corrections to Higgs boson couplings in non-minimal Higgs models. Phys. Rev. D **96**, 035014 (2017). https://doi.org/10.1103/PhysRevD.96.035014. arXiv:1705.05399
83. P. Basler, M. Mühlleitner, J. Wittbrodt, The CP-violating 2HDM in light of a strong first order electroweak phase transition and implications for Higgs pair production. JHEP **03**, 061 (2018). https://doi.org/10.1007/JHEP03(2018)061. arXiv:1711.04097
84. P. Basler, M. Mühlleitner, BSMPT (beyond the standard model phase transitions): a tool for the electroweak phase transition in extended Higgs sectors. Comput. Phys. Commun. **237**, 62–85 (2019). https://doi.org/10.1016/j.cpc.2018.11.006. arXiv:1803.02846
85. P. Basler, M. Mühlleitner, J. Müller, Electroweak phase transition in non-minimal Higgs sectors. JHEP **05**, 016 (2020). https://doi.org/10.1007/JHEP05(2020)016. arXiv:1912.10477
86. P. Basler, M. Mühlleitner, J. Müller, BSMPT v2 a tool for the electroweak phase transition and the baryon asymmetry of the universe in extended Higgs sectors. Comput. Phys. Commun. **269**, 108124 (2021). https://doi.org/10.1016/j.cpc.2021.108124. arXiv:2007.01725
87. P. Basler, L. Biermann, M. Mühlleitner, J. Müller, R. Santos, J.A. Viana, BSMPT v3 a tool for phase transitions and primordial gravitational waves in extended Higgs sectors. arXiv:2404.19037

88. J. Braathen, S. Kanemura, Leading two-loop corrections to the Higgs boson self-couplings in models with extended scalar sectors. Eur. Phys. J. C **80**, 227 (2020). https://doi.org/10.1140/epjc/s10052-020-7723-2. arXiv:1911.11507
89. H. Bahl, J. Braathen, G. Weiglein, New constraints on extended Higgs sectors from the trilinear Higgs coupling. Phys. Rev. Lett. **129**, 231802 (2022). https://doi.org/10.1103/PhysRevLett.129.231802. arXiv:2202.03453
90. H. Bahl, J. Braathen, M. Gabelmann, G. Weiglein, anyH3: precise predictions for the trilinear Higgs coupling in the standard model and beyond. Eur. Phys. J. C **83**, 1156 (2023). https://doi.org/10.1140/epjc/s10052-023-12173-8. arXiv:2305.03015
91. H. Bahl, J. Braathen, M. Gabelmann, S. Paßehr, Generic two-loop results for trilinear and quartic scalar self-interactions. arXiv:2503.15645
92. M. Krause, R. Lorenz, M. Muhlleitner, R. Santos, H. Ziesche, Gauge-independent renormalization of the 2-Higgs-doublet model. JHEP **09**, 143 (2016). https://doi.org/10.1007/JHEP09(2016)143. arXiv:1605.04853
93. F. Bojarski, G. Chalons, D. Lopez-Val, T. Robens, Heavy to light Higgs boson decays at NLO in the singlet extension of the standard model. JHEP **02**, 147 (2016). https://doi.org/10.1007/JHEP02(2016)147. arXiv:1511.08120
94. M. Krause, D. Lopez-Val, M. Muhlleitner, R. Santos, Gauge-independent renormalization of the N2HDM. JHEP **12**, 077 (2017). https://doi.org/10.1007/JHEP12(2017)077. arXiv:1708.01578
95. M. Krause, M. Mühlleitner, M. Spira, 2HDECAY – a program for the calculation of electroweak one-loop corrections to Higgs decays in the two-Higgs-doublet model including state-of-the-art QCD corrections. Comput. Phys. Commun. **246**, 106852 (2020). https://doi.org/10.1016/j.cpc.2019.08.003. arXiv:1810.00768
96. A. Denner, S. Dittmaier, J.-N. Lang, Renormalization of mixing angles. JHEP **11**, 104 (2018). https://doi.org/10.1007/JHEP11(2018)104. arXiv:1808.03466
97. M. Krause, M. Mühlleitner, ewN2HDECAY – a program for the calculation of electroweak one-loop corrections to Higgs decays in the next-to-minimal two-Higgs-doublet model including state-of-the-art QCD corrections. Comput. Phys. Commun. **247**, 106924 (2020). https://doi.org/10.1016/j.cpc.2019.106924. arXiv:1904.02103
98. M. Krause, M. Mühlleitner, Impact of electroweak corrections on neutral Higgs Boson decays in extended Higgs sectors. JHEP **04**, 083 (2020). https://doi.org/10.1007/JHEP04(2020)083. arXiv:1912.03948
99. D. Azevedo, P. Gabriel, M. Muhlleitner, K. Sakurai, R. Santos, One-loop corrections to the Higgs boson invisible decay in the dark doublet phase of the N2HDM. JHEP **10**, 044 (2021). https://doi.org/10.1007/JHEP10(2021)044. arXiv:2104.03184
100. F. Egle, M. Mühlleitner, R. Santos, J.A. Viana, One-loop corrections to the Higgs boson invisible decay in a complex singlet extension of the SM. arXiv:2202.04035
101. M.D. Goodsell, S. Liebler, F. Staub, Generic calculation of two-body partial decay widths at the full one-loop level. Eur. Phys. J. C **77**, 758 (2017). https://doi.org/10.1140/epjc/s10052-017-5259-x. arXiv:1703.09237
102. J. Baglio, C. Weiland, Heavy neutrino impact on the triple Higgs coupling. Phys. Rev. D **94**, 013002 (2016). https://doi.org/10.1103/PhysRevD.94.013002. arXiv:1603.00879
103. J. Baglio, C. Weiland, The triple Higgs coupling: a new probe of low-scale seesaw models. JHEP **04**, 038 (2017). https://doi.org/10.1007/JHEP04(2017)038. arXiv:1612.06403
104. T.N. Dao, R. Gröber, M. Krause, M. Mühlleitner, H. Rzehak, Two-loop $mathcal O(\alpha_t^2)$ corrections to the neutral Higgs boson masses in the CP-violating NMSSM. arXiv:1903.11358
105. J.A. Casas, A. Ibarra, Oscillating neutrinos and $\mu \to e\gamma$. Nucl. Phys. B **618**, 171–204 (2001). https://doi.org/10.1016/S0550-3213(01)00475-8. arXiv:hep-ph/0103065
106. E. Arganda, M.J. Herrero, X. Marcano, C. Weiland, ', Imprints of massive inverse seesaw model neutrinos in lepton flavor violating Higgs boson decays. Phys. Rev. D **91**, 015001 (2015). https://doi.org/10.1103/PhysRevD.91.015001. arXiv:1405.4300
107. T. Plehn, M. Spira, P.M. Zerwas, Pair production of neutral Higgs particles in gluon–gluon collisions. Nucl. Phys. B **479**, 46–64 (1996). https://doi.org/10.1016/0550-3213(96)00418-X. arXiv:hep-ph/9603205
108. S. Dawson, S. Dittmaier, M. Spira, Neutral Higgs boson pair production at hadron colliders: QCD corrections. Phys. Rev. D **58**, 115012 (1998). https://doi.org/10.1103/PhysRevD.58.115012. arXiv:hep-ph/9805244
109. F. Arco, S. Heinemeyer, M. Mühlleitner, Large one-loop effects of BSM triple Higgs couplings on double Higgs production at e^+e^- colliders. arXiv:2505.02947
110. J. Kublbeck, M. Bohm, A. Denner, Feyn Arts: computer algebraic generation of Feynman graphs and amplitudes. Comput. Phys. Commun. **60**, 165–180 (1990). https://doi.org/10.1016/0010-4655(90)90001-H
111. T. Hahn, Generating Feynman diagrams and amplitudes with FeynArts 3. Comput. Phys. Commun. **140**, 418–431 (2001). https://doi.org/10.1016/S0010-4655(01)00290-9. arXiv:hep-ph/0012260
112. T. Hahn, M. Perez-Victoria, Automatized one loop calculations in four-dimensions and D-dimensions. Comput. Phys. Commun. **118**, 153–165 (1999). https://doi.org/10.1016/S0010-4655(98)00173-8. arXiv:hep-ph/9807565
113. J. Elias-Miro, J.R. Espinosa, T. Konstandin, Taming infrared divergences in the effective potential. JHEP **08**, 034 (2014). https://doi.org/10.1007/JHEP08(2014)034. arXiv:1406.2652
114. S.P. Martin, Taming the Goldstone contributions to the effective potential. Phys. Rev. D **90**, 016013 (2014). https://doi.org/10.1103/PhysRevD.90.016013. arXiv:1406.2355
115. N. Kumar, S.P. Martin, Resummation of Goldstone boson contributions to the MSSM effective potential. Phys. Rev. D **94**, 014013 (2016). https://doi.org/10.1103/PhysRevD.94.014013. arXiv:1605.02059
116. J. Braathen, M.D. Goodsell, Avoiding the Goldstone boson catastrophe in general renormalisable field theories at two loops. JHEP **12**, 056 (2016). https://doi.org/10.1007/JHEP12(2016)056. arXiv:1609.06977
117. J. Braathen, M.D. Goodsell, F. Staub, Supersymmetric and non-supersymmetric models without catastrophic Goldstone bosons. Eur. Phys. J. C **77**, 757 (2017). https://doi.org/10.1140/epjc/s10052-017-5303-x. arXiv:1706.05372
118. Particle Data Group Collaboration, R.L. Workman et al., Review of particle physics. PTEP **2022**, 083C01 (2022). https://doi.org/10.1093/ptep/ptac097
119. H. Bahl, T. Biekötter, S. Heinemeyer, C. Li, S. Paasch, G. Weiglein et al., HiggsTools: BSM scalar phenomenology with new versions of HiggsBounds and HiggsSignals. Comput. Phys. Commun. **291**, 108803 (2023). https://doi.org/10.1016/j.cpc.2023.108803. arXiv:2210.09332
120. P. Bechtle, D. Dercks, S. Heinemeyer, T. Klingl, T. Stefaniak, G. Weiglein et al., HiggsBounds-5: testing Higgs sectors in the LHC 13 TeV era. arXiv:2006.06007
121. P. Bechtle, S. Heinemeyer, T. Klingl, T. Stefaniak, G. Weiglein, J. Wittbrodt, HiggsSignals-2: probing new physics with precision Higgs measurements in the LHC 13 TeV era. Eur. Phys. J. C **81**, 145 (2021). https://doi.org/10.1140/epjc/s10052-021-08942-y. arXiv:2012.09197
122. L. Shang, Y. Zhang, EasyScan_HEP: a tool for connecting programs to scan the parameter space of physics models. Comput.

Phys. Commun. **296**, 109027 (2024). https://doi.org/10.1016/j.cpc.2023.109027. arXiv:2304.03636

123. M. Mühlleitner, D.T. Nhung, H. Rzehak, K. Walz, Two-loop contributions of the order $\mathcal{O}(\alpha_t\alpha_s)$ to the masses of the Higgs bosons in the CP-violating NMSSM. JHEP **05**, 128 (2015). https://doi.org/10.1007/JHEP05(2015)128. arXiv:1412.0918